4

Volcanism on the Red Planet: Mars

Ronald Greeley, Nathan T. Bridges, David A. Crown, Larry Crumpler, Sarah A. Fagents, Peter J. Mouginis-Mark, and James R. Zimbelman

4.1. INTRODUCTION

Of all of the planets in the solar system, Mars is the most Earth-like in its geologic characteristics. Like Earth, it has been subjected to exogenic processes, such as impact cratering and erosion by wind and water, as well as endogenic processes, including tectonic deformation of the crust and volcanism. The effects of these processes are amply demonstrated by the great variety of surface features, including impact craters, landslides, former river channels, sand dunes, and the largest volcanoes in the solar system.

Some of these features suggest substantial changes in Mars' environment during its history. For example, as reviewed by Carr (1996), today Mars is a cold, dry desert with an average atmospheric pressure of only 5.6 mbar, which does not allow liquid water to exist on the surface. To some planetary scientists, the presence of the channels bespeaks a time when Mars was warmer and wetter. However, others have argued that these features might have formed under current conditions and that there might not have been a shift in climate.

Could the morphology of volcanoes and related features provide clues to past Martian environments? What role is played by atmospheric density in the styles of eruptions on Mars and resulting landforms? If these and related questions can be answered, then we may have a means for assessing the conditions on Mars' surface in the past and comparing the results with models of Martian evolution.

In this chapter, we outline the sources of information available for volcanism on Mars, explore the influence of the Martian environment on volcanic processes, and describe the principal volcanic features and their implications for understanding the general evolution of the Martian surface.

Environmental Effects on Volcanic Eruptions: From Deep Oceans to Deep Space.
Edited by Zimbelman and Gregg, Kluwer Academic/Plenum Publishers, New York, 2000.

4.2. BACKGROUND

Earth-based telescopic observations are unable to resolve volcanoes on Mars. However, even before volcanic features were identified in spacecraft images, astronomers noted the presence of a unique W-shaped cloud in the Tharsis region that developed around local noon and persisted through the afternoon. This cloud was "anchored" to what we now know are three enormous volcanoes. The first identification of these volcanoes came early in the Mariner 9 mission in 1971 (McCauley *et al.*, 1972). A massive global dust storm obscured the entire surface when the spacecraft arrived at Mars. As the dust slowly settled, four dark "spots" in the Tharsis region were revealed to be the summits of Olympus Mons, perhaps the largest volcano in the solar system, and the Tharsis Montes (Masursky *et al.*, 1972; Carr, 1973). By the end of the mission, additional volcanoes were identified throughout the Tharsis and Elysium regions, as well as in the southern highlands (Figure 4.1). Cameras on two Viking Orbiter spacecraft operated at Mars from 1976 to 1980, greatly improving our understanding of these and other volcanoes (Figure 4.2), as well as revealing extensive volcanic plains (Figure 4.3), small volcanoes in many areas, including the cratered highlands, and other features related to volcanic processes (Carr *et al.*, 1977).

Much of the understanding of Martian volcanoes has been derived from photogeologic studies of the surface. Through careful mapping, the global geology of Mars is now well established (Carr, 1981; Scott and Tanaka, 1986; Greeley and Guest, 1987; Tanaka and Scott, 1987). The areal density of impact craters on the mapped units allows a relative stratigraphy to be determined even where units are not in contact. The three major divisions for Mars' geologic history are the Noachian (oldest), Hesperian, and Amazonian (youngest) Periods.

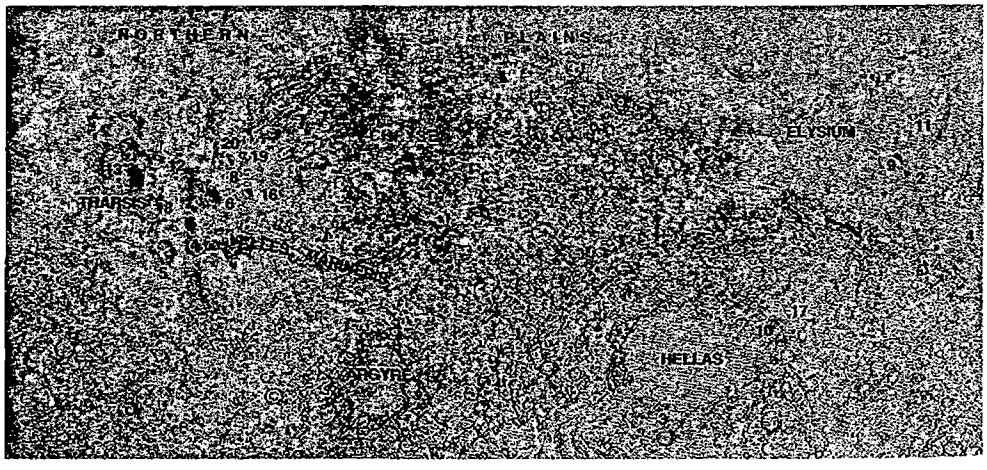

Figure 4.1. Shaded airbrush relief map of Mars (from 65 °N to 65 °S) showing the location of principal volcanic features. 1, Alba Patera; 2, Albor Tholus; 3, Amphitrites Patera; 4, Apollinaris Patera; 5, Arsia Mons; 6, Ascraeus Mons; 7, Biblis Patera; 8, Ceraunius Tholus; 9, Elysium Mons; 10, Hadriaca Patera; 11, Hecates Tholus; 12, Jovis Tholus; 13, Olympus Mons; 14, Pavonis Mons; 15, "Tempe" Patera; 16, Tharsis Tholus; 17, Tyrrhena Patera; 18, Ulysses Patera; 19, Uranius Patera; 20, Uranius Tholus. In addition, many of the plains portrayed here are thought to be of volcanic origin. From Greeley and Spudis (1981).

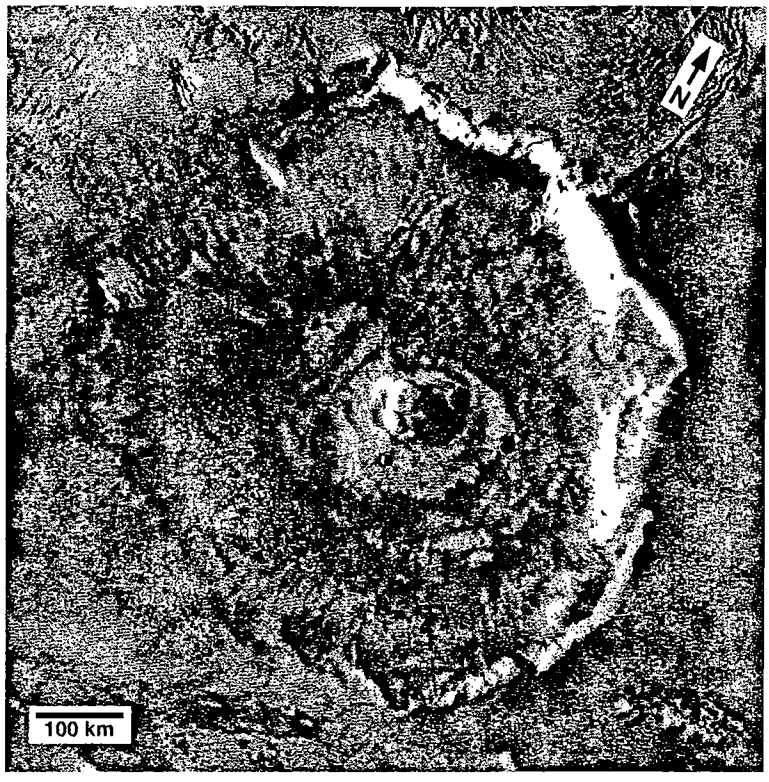

Figure 4.2. The shield volcano Olympus Mons is more than 600 km across. It is constructed from countless individual flows erupted from the summit region and the flanks of the volcano. (Viking Orbiter frame 646A28.)

Unfortunately, the absolute ages are poorly constrained; for example, different models of the impact cratering rate allow the start of the Amazonian Period to be from millions (e.g., Soderblom, 1977) to billions (e.g., Neukum and Hiller, 1981) of years in age. The ages will remain unconstrained until radiometric dates are obtained (probably from rock samples returned to Earth) for relevant stratigraphic units on Mars. Despite the uncertainty in absolute age, the stratigraphy provides a framework within which relative ages can be constrained, including those of volcanic features.

Other types of remote sensing provide information about Martian volcanoes that is complementary to photogeologic studies. Earth-based telescopic reflectance spectra indicate that bright regions are covered with dust rich in oxidized iron, whereas dark regions are less dusty and may include pyroxene-bearing mafic rocks such as basalt (Soderblom, 1992). Thermal infrared measurements by the Viking Orbiters suggest that much of the surface is coated with fine-grained material ranging from micrometer-sized dust covering bright regions to sand-sized particles mixed with larger materials in dark regions (Kieffer *et al.*, 1977). The dust coating also affects individual volcanoes, where dust might interfere with reflectance or emission from the underlying rocks, hindering remote sensing interpretations of bedrock compositions.

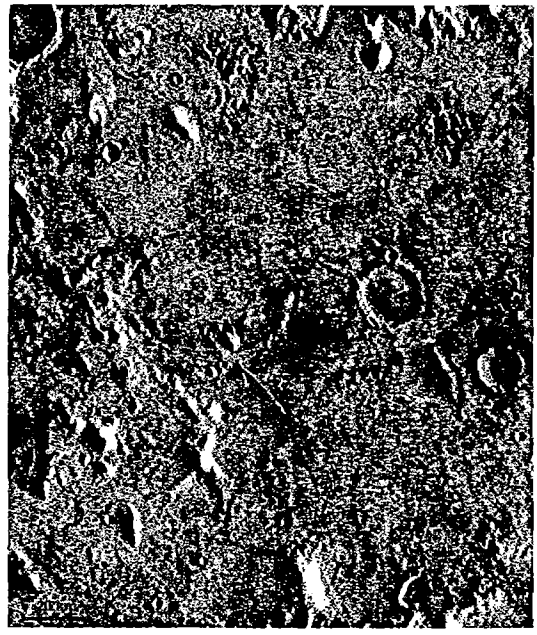

Figure 4.3. Volcanic plains have "resurfaced" many areas of Mars, including cratered terrain seen here northwest of the Hellas basin where lava flows have partly buried older craters. Area shown is about 170 by 150 km. (Viking Orbiter frame 95A10.)

4.3. MARS' COMPOSITION

Composition strongly affects the rheology and explosivity of magmas and lavas. As such, it must be considered to understand Martian volcanology.

4.3.1. Bulk Composition

The mass and volume of Mars are well known and yield a mean uncompressed planetary density of 3933.5 ± 0.4 kg m^{-3}. This is considerably lower than Earth's density of 5514.8 kg m^{-3}, implying that Mars' interior (core + mantle) is depleted in heavy elements, such as Fe, relative to light elements such as O, Mg, Si, and S. Further insight into Mars' composition comes from the class of meteorites known as SNCs (for the meteorites shergottites, nakhlites, and Chassigny). These basaltic to ultramafic rocks are considered to be of Martian origin based on the compositional similarity of their trapped gases to Mars' atmosphere (McSween, 1994). Although they probably do not completely represent volcanic rocks on Mars, the inferred SNC parent magmas share geochemical and isotopic characteristics that suggest melting of the same mantle source at various times (McSween, 1994). SNCs are enriched in iron relative to magnesium, which may indicate formation from evolved liquids, but can also be traced to an iron-rich mantle.

Mars' polar moment of inertia of 0.3662 ± 0.0017 suggests that it has a differentiated interior (Folkner *et al.*, 1997). Although several nonunique models that consider core size, mantle and core compositions, and temperature gradient can reproduce the observed moment of inertia, the best model involves a core ranging in composition from Fe to FeS that is a

smaller fraction of the planetary mass than is Earth's core. The Martian mantle would contain the remainder of the iron and be more iron-rich than Earth's mantle (Table 4.1). The mineralogy of the upper mantle is probably lherzolitic, made up of olivine, pyroxene, and minor aluminum phases (Longhi *et al.*, 1992). This is similar to Earth's upper mantle, except that on Mars the mafic minerals would be more iron-rich. Combining the iron contents of the small Martian core and iron-rich mantle results in a total iron content that is less than that of the bulk Earth.

4.3.2. Remote Sensing

Remote sensing of Mars divides the surface into ferric-rich (oxidized) bright regions and ferrous-rich dark regions (Bell, 1996). Broad, weak absorption bands from 9.0 to 1.1 μm in the dark regions are interpreted as Fe^{2+} cations in pyroxene and olivine. Infrared absorption indicative of sulfates and possibly carbonates on the surface and in atmospheric dust is also apparent (Blaney and McCord, 1990, 1995; Pollack *et al.*, 1990; Soderblom, 1992). Additional information provided by the Mars Global Surveyor spacecraft about thermal emission features in some dark regions indicates abundant pyroxene and plagioclase, and limits the amount of olivine, quartz, carbonates, and clays to be no more than 10, 5, 10, and 20% of the surface, respectively (Christensen *et al.*, 1998). Mineralogic OH^- or H_2O has been observed in the near infrared, but the associated mineralogy is uncertain (Bell, 1996).

The ferrous–ferric heterogeneity observed from Earth and orbit is also seen on the surface. Spectra from the visible–near-infrared Imager for Mars Pathfinder (IMP) camera indicate the presence of three classes of rocks and four classes of soils (Smith *et al.*, 1997; McSween *et al.*, 1999). Many of the diagnostic spectral characteristics of the classes are explained by differences in the abundance of ferric (high red/blue ratio) and ferrous (low red/blue ratio) components.

The morphology of volcanic features provides some insight into surface chemistry. The appearance of most volcanoes and lava flows is consistent with low-viscosity basaltic volcanism (Blasius and Cutts, 1981; Hodges and Moore, 1994). Attempts to derive compositionally dependent parameters by matching flow morphology to rheology suggest compositions ranging from basalt to andesite (Hulme, 1976; Malin, 1977; Moore *et al.*, 1978; Zimbelman, 1985). Landforms suggestive of silicic volcanism are represented by a few highland structures resembling volcanic domes, a possible composite volcano (Greeley and Spudis, 1978), and festooned flows (Fink, 1980; Hodges and Moore, 1994).

4.3.3. *In Situ* Measurements

In situ measurements of the elemental composition of Martian surface materials were made by the Viking X-ray Fluorescence Spectrometer (XRF) and the Pathfinder/Sojourner Alpha Proton X-ray Spectrometer (APXS). *In situ* mineralogy was also inferred from the Pathfinder magnetic properties experiments. The soils at the Viking and Pathfinder sites are similar, although the soils at the Pathfinder site are somewhat depleted in S and enriched in Ti (Table 4.1; Banin *et al.*, 1992; Rieder *et al.*, 1997). The soils have compositions comparable to those of palagonite, a hydrated volcanic glass, and could represent the weathered products of basaltic rocks. The abundant S and Cl may be derived from volcanic gases that reacted with the surface (Banin *et al.*, 1992). The Pathfinder magnetic properties experiments indicate that the magnetized component of Martian dust is composed of claylike aggregates stained or cemented by Fe_2O_3. Some of the ferric oxide is probably maghemite ($g\text{-}Fe_2O_3$) formed by the

Table 4.1. Compositions of Martian Materials and Comparisons with Earth[a]

Name	SiO_2	TiO_2	Al_2O_3	MgO	FeO	CaO	Na_2O	K_2O	MnO	Cr_2O_3	P_2O_5	SO_3	Cl	Fe_2O_3	Reference
Pathfinder soils[b]															
A-2	51	1.2	7.4	7.9	16.6	6.9	2.3	0.2				4	0.5		Rieder *et al.* (1997)
A-4	48	1.4	9.1	8.3	14.4	5.6	3.8	0.2				6.5	0.6		Rieder *et al.* (1997)
A-5	47.9	0.9	8.7	7.5	17.3	6.5	2.8	0.3				5.6	0.6		Rieder *et al.* (1997)
A-8	51.6	1.1	9.1	7.1	13.4	7.3	2	0.5				5.3	0.7		Rieder *et al.* (1997)
A-10	48.2	1.1	8.3	7.9	17.4	6.4	1.5	0.2				6.2	0.7		Rieder *et al.* (1997)
A-15	50.2	1.3	8.4	7.3	17.1	6	1.3	0.5				5.2	0.6		Rieder *et al.* (1997)
Pathfinder rocks[b]															
A-3	58.6	0.8	10.8	3	12.9	5.3	3.2	0.7				2.2	0.5		Rieder *et al.* (1997)
A-7	55.5	0.9	9.1	5.9	13.1	6.6	1.7	0.5				3.9	0.6		Rieder *et al.* (1997)
A-16	52.2	1	10	4.9	15.4	7.4	3.1	0.7				2.8	0.5		Rieder *et al.* (1997)
A-17	61.2	0.7	9.9	3	11.9	7.8	2	0.5				0.7	0.3		Rieder *et al.* (1997)
A-18	55.3	0.9	10.6	4.9	13.9	6	2.4	0.8				2.6	0.6		Rieder *et al.* (1997)
Pathfinder "soil-free" rock[b]															
	62	0.7	10.6	2	12	7.3	2.6	0.7				0	0.2		Rieder *et al.* (1997)
Average Viking soils[c]															
	43	0.6	7.2	6		5.8						7.2	0.6	18	Banin *et al.* (1992)
SNC bulk															
Zagami	51.2	0.81	6.19	10.4	18.2	10.7	1.29	0.13	0.55		0.58				McCoy *et al.* (1992)
SNC meteorite parental magma estimates															
Nakhla (NK93)	50.2	1.0	8.6	4.0	19.1	11.9	1.2	2.8	0.4	0.1	0.7				Treiman (1993)
Nakhla (GV1)	46.7	4.2	8.1	5.1	23.3	9.7	2.1	1.2							Harvey and McSween (1992)

Nakhla (NK3)	45.8	3.1	7.2	5.7	26.2	10.4	0.8	1.4			Harvey and McSween (1992)
Nakhla (N)	48.9	1.1	2.8	5.2	26.1	13.8	1.0	0.2	0.7	0.1	Longhi and Pan (1989)
Chassigny	51.52	1.58	8.72	7.08	19.02	8.49	2.29	0.77	0.53		Johnson *et al.* (1991)
Mars mantle + crust models[d]											
1	36.8	0.2	3.1	29.9	26.8	2.4	0.2		0.1	0.4	BVTP (1981)
2	40	0.1	3.1	27.4	24.3	2.5	0.8		0.2	0.6	Anderson (1972)
3	43.9	0.16	3.2	31.2	16.7	3	1.4				Weidenschilling (1976)
4	41.6	0.3	6.4	29.8	15.8	5.2	0.1		0.15	0.6	Morgan and Anders (1979)
5	39.4	0.6	3.1	32.7	20.8	2.7	0.5				McGetchin and Smyth (1978)
6	44.4	0.1	3	30.2	17.9	2.4	0.5		0.5	0.8	Dreibus and Wanke (1985), Longhi *et al.* (1992)
Earth mantle + crust model[d]											
	45.1	0.2	4	38.3	7.8	3.5	0.3		0.1	0.5	Jagoutz *et al.* (1979)

[a] Expressed in weight percent.
[b] Compositions normalized to a sum of 98%. Errors associated with each oxide can be found in Rieder *et al.* (1997).
[c] Compositions normalized to a sum of 95.4%.
[d] The Mars and Earth mantle + crust models come from Table 1 in Longhi *et al.* (1992). Model 1: 30% Orgueil C1 chondrite + 70% high-temperature component; model 2: mixture of chondrites; model 3: modified equilibrium condensation; model 4: four-component meteorite model; model 5: pyrolite + FeO; model 6: based on SNC data.

leaching of Fe^{2+} from rock by liquid water (Hviid *et al.*, 1997), followed by oxidation and precipitation.

Data from five rocks at the Pathfinder site reveal a composition rich in Si and K and depleted in Mg relative to the soils and SNC meteorites (Figure 4.4). The rock chemistry is similar to that of icelandite, an anorogenic andesite (Figure 4.5; McSween *et al.*, 1999). This composition closely mirrors that of the average composition of Earth's continental crust, except for a higher iron content, which may be related to the greater abundance of Fe thought to exist in the Martian mantle (Table 4.1). The S content of the rocks is unusually high for a primary igneous composition because it exceeds the S solubility in most magmas and common volcanic rocks (Rieder *et al.*, 1997; McSween *et al.*, 1999). There is a strong correlation between the red/blue ratio derived from IMP spectra and S content, suggesting contamination by dust derived from sulfur-rich, red soil (Bridges *et al.*, 1997). Subtracting S from the rock composition by adjusting the other elements according to regressions of each element versus S indicates that the rock could contain as much as 62% SiO_2 (Rieder *et al.*, 1997; McSween *et al.*, 1999).

4.3.4. Implications

From the various data sources, we can summarize the likely compositions of Martian volcanoes and lava flows. SNC parent magmas have low alumina and high iron [Fe/(Fe + Mg)] contents relative to terrestrial basalts and in some respects more closely resemble basaltic komatiites (McSween, 1994). Basaltic shergottites probably represent

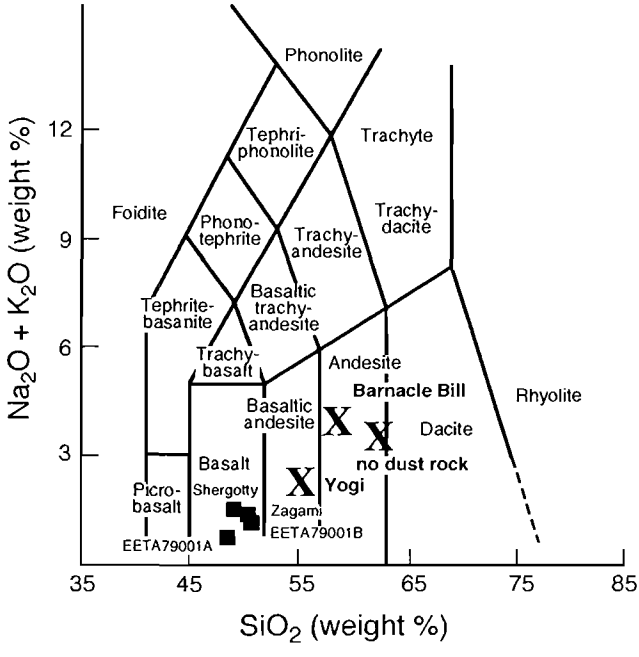

Figure 4.4. Weight percent alkalis versus silica for representative Pathfinder rocks (X, including Barnacle Bill) and SNC meteorites (squares). The "no dust" rock composition is found by plotting linear regressions of each oxide versus sulfur and then extrapolating to zero percent S.

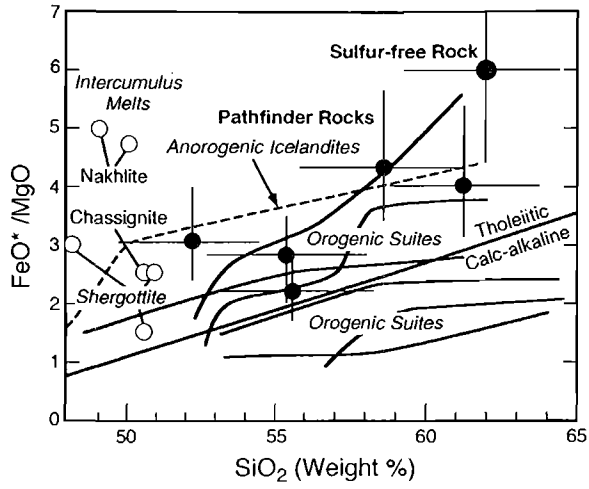

Figure 4.5. FeO*/MgO versus silica for Pathfinder rocks, SNC meteorites, and terrestrial igneous associations. Tholeiitic and calc-alkaline differentiation trends that result in andesites are shown (trends from Gill, 1981). Pathfinder rocks plot along a tholeiitic trend and have compositions close to those of anorogenic icelandites. The label "FeO*" is used to recognize that all Pathfinder iron analyses are reported as FeO even though some Fe_2O_3 is probably present. From McSween *et al.* (1998).

shallow intrusive rocks or thick lava flows that contained suspended crystals (McCoy *et al.*, 1992; McSween, 1994). The morphology of most volcanoes and lava flows is consistent with low-viscosity, basaltic compositions. If the compositions measured by the Pathfinder APXS represent igneous rocks and are not strongly affected by chemical weathering, then andesites may also be present on Mars.

Although knowledge of Martian geochemistry is incomplete, it can provide insight into volcanic processes on Mars. The best estimates of physical properties of mafic Martian lavas come from analyses of the SNC meteorites. The viscosities of crystal-free, liquidus SNC magmas range from a few to tens of pascals seconds and can be even lower if dissolved water is present. These values are similar to the liquidus viscosities of terrestrial and lunar basalts. The average density of SNC parent magmas might be slightly greater (by ~5%) than those of terrestrial basalts (McSween, 1994). The lack of Martian rock samples of more evolved compositions precludes estimates of their physical properties.

An important factor controlling the viscosity and bulk density of lava is the volatile content, which affects magma ascent rate, vesicle abundance, bulk density, and viscosity. Unfortunately, the amount of water in the SNC parent magmas and the Martian mantle is unknown. The bulk water content of SNCs is 130–350 ppm, lower than most terrestrial basalts (Figure 4.6). Carr and Wanke (1992) used this value to estimate a Martian mantle water content of 35 ppm, drier than estimates for the terrestrial mantle, which range up to 10^2 ppm or more (e.g., Wood *et al.*, 1996; Dreibus *et al.*, 1997). However, if kaersutite amphiboles in SNC meteorites are water-bearing, SNC parent magmas may have contained up to 1.4 wt% H_2O after kaersutite crystallization and 4 wt% prior to crystallization (Johnson *et al.*, 1991; McSween and Harvey, 1993). If the kaersutites are H-deficient (Popp *et al.*, 1995), then the amount of water in the magma is uncertain.

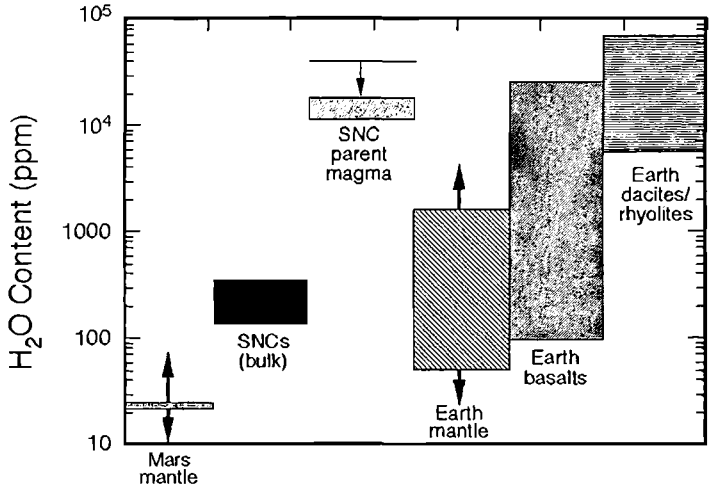

Figure 4.6. Water contents of Martian and terrestrial materials. Mantle values represent a range of estimates; the horizontal line represents the possible water content of the SNC parent mantle source prior to kaersutite crystallization. Bulk SNC and possible parent SNC water contents are from McSween and Harvey (1993) and McSween (1994). Earth basalt and dacite/rhyolite values are from compilations by Johnson *et al.* (1994) and Clemens (1984).

4.4. INFLUENCE OF MARS' ENVIRONMENT ON VOLCANISM

Many factors influence the styles of volcanic eruptions (Whitford-Stark, 1982) and the resulting volcanic morphology (Greeley, 1977; Wilson and Head, 1983). In addition to magma composition, the physical environment of Mars (Table 4.2) influences volcanic activity. For example, Mars is about half the diameter of Earth but possesses some of the largest volcanoes in the solar system. Smaller bodies cool more efficiently, so Mars probably developed a thicker lithosphere than Earth (Schubert *et al.*, 1992), perhaps accounting for the absence of plate tectonics on Mars. In turn, lack of relative motion between the lithosphere and magma source regions could have facilitated edifice construction to the large sizes observed. Furthermore, the lower mass of Mars, lower gravitational acceleration, low-density atmosphere, and cooler surface and atmosphere, work together to influence almost every aspect of ascent, storage, eruption, and emplacement of Martian magmas.

Table 4.2. Comparative Planetary Environmental Characteristics[a]

Planet	Radius (km)	Density ($kg\,m^{-3}$)	Gravity ($m\,s^{-2}$)	Atmospheric pressure (Pa)	Atmospheric density ($kg\,m^{-3}$)	Surface temperature (K)	Atmospheric composition
Mars	3390	3930	3.73	7×10^3	0.162	225	>95% CO_2, N_2,Ar,O_2
Earth	6380	5510	9.81	$\sim 10^5$	1.23	288	75% N_2 23% O_2, Ar, CO_2
Venus	6050	5160	8.88	$\sim 10^7$	70	~745	>96% CO_2, N_2,SO_2,Ar,CO
Moon	1730	3340	1.62	—	—	~240	—

[a] Atmospheric characteristics given for mean planetary radii on Mars and Venus, and for sea level standard temperate atmosphere on Earth. Temperatures are average diurnal/seasonal values.

4.4.1. Magma Ascent

The ascent of magma is driven by buoyancy, which is a function of diapir volume, V, acceleration related to gravity, g, and the contrast between the density of the country rock, r_r, and magma, r_m, such that the buoyancy force is given by $F_b = g(r_r - r_m)V$. Assuming that density contrasts are similar for terrestrial and Martian mafic magmas, the low gravity of Mars implies a smaller buoyancy force and, hence, a smaller rise velocity for a given magma viscosity. To avoid cooling and solidification during ascent, rising magma bodies on Mars must be larger than on Earth (Wilson and Head, 1994). Rising magma can stall at rheologic barriers such as the asthenosphere–lithosphere boundary or the brittle–ductile transition at the base of the elastic lithosphere, or at a density barrier, at which buoyancy forces are reduced to zero as the country rock density decreases toward the surface (Rubin and Pollard, 1987). In both instances, magma ascent may continue through dikes as a result of brittle fracture of the country rock in response to stresses imposed by the magma body. A thick lithosphere on Mars would imply deeper rheologic barriers. In the case of neutral buoyancy zones, development of excess pressure in the magma reservoir (e.g., as a result of continued magma input or gas exsolution) could initiate dike propagation.

Consideration of gravity and compaction of Martian crustal rock suggests that neutral buoyancy zones and magma reservoirs should be deeper on Mars than on Earth (Wilson and Head, 1994). For magma to reach the surface from deep rheologic or density traps, wider dikes and greater driving pressures are required. Fracture mechanics suggests that the dimensions of dikes are inverse functions of planetary gravity (Wilson and Head, 1994). Thus, dikes on Mars should be larger and accommodate greater magma velocities. Furthermore, large magma reservoirs, inferred from both theory and the large sizes of many Martian calderas (Wood, 1984; Crumpler *et al.*, 1996b) and lava flows (Cattermole, 1987), should maintain greater driving pressures for longer durations. Together, these influences on magma motion imply systematically greater eruption rates and individual eruption volumes than on Earth.

4.4.2. Role of Volatiles

Volatiles such as H_2O and CO_2 contained in the magma are important to the style of eruption. Volatile solubility is partly a function of pressure, so as pressure decreases during magma ascent, bubbles of gas nucleate and grow by diffusion, decompression, and coalescence (Sparks, 1978). If the gas occupies a sufficiently large volume, the magma will disrupt into fragments entrained in a gas stream, resulting in explosive eruptions. The total pressure, P, at any depth, z, in the lithosphere is equal to the sum of the lithostatic and external atmospheric pressures. Thus, the low Martian gravity and atmospheric pressure combine to ensure that $P(z)$ is less than that on Earth. This has important implications for magmatic volatiles. Because of the lower pressure in the Martian lithosphere, and the lower lithostatic pressure gradient, the levels at which volatile exsolution and magma fragmentation occur are deeper and more widely separated than on Earth allowing the growth of multiple bubble populations (Wilson *et al.*, 1982). If the volatile content exceeds ~0.03 wt% H_2O (300 ppm) or a few ppm CO_2 (values significantly lower than for Earth), the expected result is a highly fragmented magma. After release by fragmentation, gas expansion is augmented by the low atmospheric pressure on Mars, which permits a greater energy release per unit mass, leading ultimately to greater eruption velocities (Wilson *et al.*, 1982).

4.4.3. Explosive Eruptions

On Earth, explosive basaltic eruptions are commonly weak because the low volatile content and viscosity of basalt produces coarsely fragmented magma erupted at low speeds, forming small lava fountains. Typically, clast ponding occurs to form lava flows; spatter and scoria deposits may also form, depending on eruption conditions. On Mars, the predicted high eruption velocities and efficient energy transfer between fine pyroclasts and the gas suggest that vigorous Plinian eruptions might have been common, even though they are rare for terrestrial basalts. In such eruptions, the emerging volcanic jet entrains and heats atmospheric gas such that the bulk density of the expanding gas–particle mixture may become less than the density of the atmosphere, promoting buoyant ascent of a tall, convecting eruption column (Wilson *et al.*, 1978). The greater eruption velocity, together with differences in atmospheric temperature and pressure, would produce columns several times higher than on Earth. However, the limited expansion potential of low-density atmospheric gas means that buoyancy is not so readily achieved, so that unstable fountains that collapse to feed pyroclastic flows would be more common than on Earth (Wilson *et al.*, 1982). Although pyroclastic flows have been tentatively identified on Mars, predictions of flow distances are hampered by incomplete understanding of their emplacement mechanisms, and poor knowledge of Martian topography. To first order, the higher initial velocities and weaker particle frictional interaction (caused by low gravity; Crown and Greeley, 1993) suggest systematically greater runout distances.

The nature of a pyroclastic deposit is a function of the accumulation rate and temperature of the pyroclasts on landing. These factors are related to the structure of the erupting plume or fountain, the sizes of pyroclasts, and ultimately to the volatile content and mass eruption rate of the magma (Head and Wilson, 1989). Pyroclasts ejected into the Martian atmosphere experience little drag in comparison with Earth because aerodynamic drag is a function of atmospheric density. Together with the reduced gravitational settling and initial high eruption velocities on Mars, this implies that pyroclasts will have long trajectories, allowing significant cooling during flight. Thus, Martian explosive volcanism should result in widely dispersed, poorly consolidated deposits of fine material, forming broad, low-relief edifices. If volatile-poor eruptions produce coarser clasts, they may form lava fountains, which would be taller and wider than those on Earth (Wilson and Head, 1994). The coarsest clasts would accumulate close to the vent to form flows and spatter deposits, but smaller clasts would follow long trajectories, cooling and forming broad deposits of scoria. This might explain the apparent lack of steep cinder cones on Mars (Wood, 1979; Edgett, 1990).

4.4.4. Role of Ground Water/Ice

The probable existence of ice in the regolith at higher latitudes (Clifford, 1993) and the postulated warmer, wetter climate in the past (Owen, 1992) imply ample opportunity for magma/water interactions. These could include melting and release of ground water by intrusions or lava flows, explosive generation of rootless "pseudocraters" by lavas flowing over a saturated substrate, increased eruptive vigor in sustained explosive eruptions, and formation of explosion craters (e.g., maars). Volcano/ice interactions on Mars are discussed in Chapter 3.

Some volcanic features suggestive of ground water release have been proposed for Mars (Frey *et al.*, 1979; Mouginis-Mark *et al.*, 1982, 1988; Mouginis-Mark, 1985; Squyres *et al.*, 1987; Greeley and Crown, 1990; Crown and Greeley, 1993). However, the apparent scarcity of identified maars might be related to the difficulty of distinguishing explosion craters from

impact craters. Models for transient explosions, in which steam is pressurized beneath a cap rock, predict ejection of clasts of country rock and juvenile magma at greater velocities than on Earth as a result of enhanced gas expansion. The higher velocities, low atmospheric drag, and low gravity suggest dispersal ranges of tens to hundreds of kilometers (Fagents and Wilson, 1996), and it is unlikely that an edifice or detectable deposit would be produced.

4.4.5. Effusive Eruptions

If magma fragmentation does not occur and the magma erupts effusively, the low gravity on Mars would lead to thicker flows, which suggests that with sufficient volumes, lavas would flow greater distances before cooling (Wilson and Head, 1994). Longer flows are also implied by the high effusion rates (Walker, 1973) and total volumes (Malin, 1980) predicted as a result of planetary environmental differences (see Section 4.1). On Earth, high effusion rates are characterized by sheetlike flows fed by long fissure vents. Low effusion rates commonly produce tube-fed lavas. These morphologies are observed on Mars, as described below.

The total heat flux from the surface of a subaerially emplaced lava is a combination of radiative, forced, and natural convective heat fluxes. The convective terms are dependent on gravity and thermal properties of the atmospheric gas, which depend on atmospheric density and viscosity. Convective heat loss should be less significant on Mars than on Earth because of differences in thermal parameters, with radiation being the dominant cooling mechanism. However, the total heat flux is somewhat less than on Earth because of the inefficiency of convective heat transfer, allowing Martian lava surface temperatures to remain tens of degrees hotter than their terrestrial counterparts for a year or more after eruption (Wilson and Head, 1994). Because of the extreme temperature dependence of lava rheology, this may enable Martian lava to remain mobile longer.

4.4.6. Summary

Unless volatile contents of Martian magmas were very low, explosive activity should have been common on Mars, forming broad, low-relief constructs. The possibility of interaction with ground water/ice enhances this probability. Because of Mars' unique environment, there is no need to invoke magmas of more evolved compositions to explain explosive features, although large Martian magma chambers could promote the generation of small volumes of more evolved magma via fractional crystallization. There are some indications that explosive activity may commonly have accompanied the extensive effusions. For example, the "stealth" terrain (Muhleman *et al.*, 1991; Edgett *et al.*, 1997), the dune fields west of the Tharsis volcanoes (Edgett, 1997), and the fine "dust" that apparently mantles many effusive features could all have explosive volcanic origins. In any case, Mars' large edifices, voluminous flows, and inferred pyroclastic deposits are consistent with predictions of larger magma chambers and dikes, greater eruption rates and volumes, and vigorous, explosive activity.

4.5. LARGE SHIELD VOLCANOES

4.5.1. Tharsis Region

The best-known volcanoes and greatest concentration of central-vent constructs occur in the Tharsis region (Figure 4.1). The Tharsis volcanoes have morphologies typical of basaltic

shield volcanoes on Earth, but are much larger. The largest, Olympus Mons, is >500 km across and 25 km high. As measured from the seafloor, Mauna Loa volcano is the largest mountain on Earth, yet it is dwarfed by the Martian volcanoes. The flanks of the Martian volcanoes have maximum slopes of 5° with shallower summit and basal slopes, similar to the subaerial part of Mauna Loa volcano. The flanks of Olympus Mons are composed of interwoven lava flows that spill onto the surrounding plains. Many of the flows have medial lava channels and partly collapsed lava tubes similar to those on terrestrial volcanoes (Greeley, 1973; Carr and Greeley, 1980). The forms and dimensions of individual flows suggest basaltic compositions, although basaltic andesite is a viable alternative (e.g., Moore *et al.*, 1978). Some of the flows and lower flanks of the Tharsis volcanoes are buried by plains-forming flows erupted from the shields or other vents (Scott and Tanaka, 1986).

Olympus Mons is surrounded by a scarp 3 to 6 km high (Figure 4.2), the origin of which is controversial. Enormous fan-shaped deposits northwest of the volcano are interpreted as landslides, perhaps lubricated by volatiles along the detachment surface (e.g. Tanaka, 1985).

Other volcanoes in the Tharsis area include *tholi* (Figure 4.7) and the unique feature Alba Patera, discussed below. Tholi are commonly smaller than 200 km in diameter and have

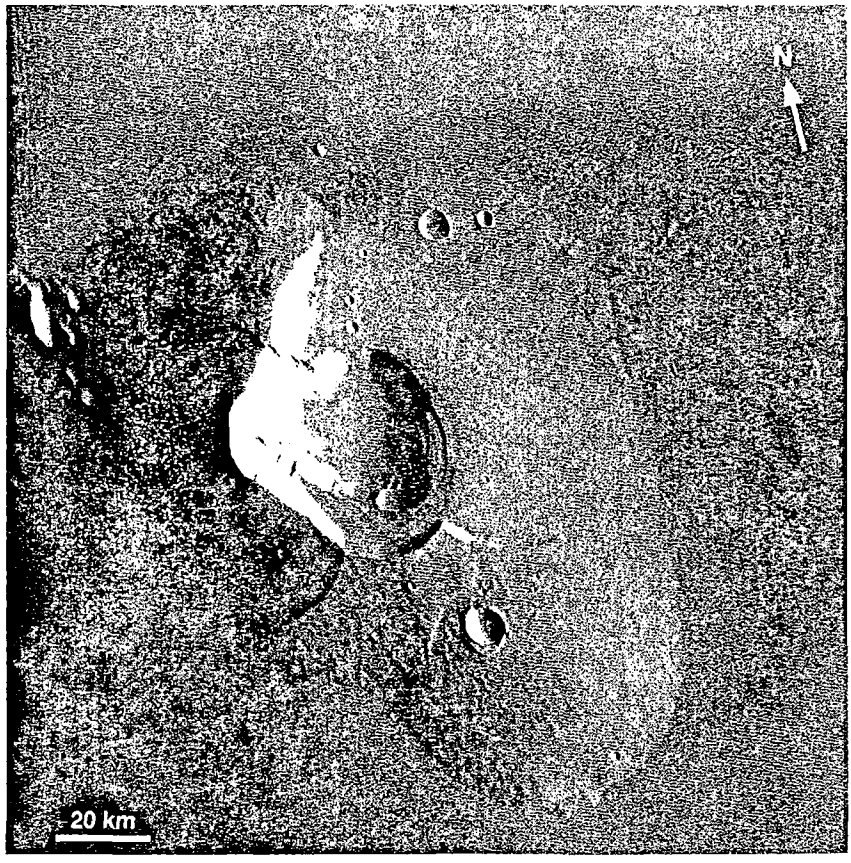

Figure 4.7. Multiple episodes of flank collapse at the summit of Tharsis Tholus may have been caused by failure of an unconsolidated basal layer equivalent to the lower units of Olympus Mons and Apollinaris Patera. The isolated massifs northwest of the cone may be large slump blocks that are embayed by lava flows from Ascraeus Mons to the west. (Viking Orbiter frame 858A23.)

a variety of morphologies. Most tend to have slopes steeper than those on the shields and have calderas more than half as wide as the overall construct, suggesting that they may be the summits of partly buried volcanoes. Ceraunius Tholus displays sinuous channels carved into its flanks, interpreted to be caused by erosive pyroclastic flows (Reimers and Komar, 1979).

4.5.2. Elysium Region

The Elysium region is also a central-vent volcanic province on Mars. Two Elysium volcanoes were compared with constructs in the Tibesti highlands in Africa (Malin, 1977) and illustrate contrasting morphologies. Hecates Tholus is ~160 by 175 km wide and ~6 km high and its flanks are cut by narrow, shallow valleys. Elysium Mons is 500 by 700 km wide and ~13 km high and displays numerous flank flows (Figure 4.8). Differences in the numbers of superposed impact craters around the summit of Hecates Tholus, including a near absence of craters within a semiannulus 2 km west of the summit (Figure 4.9), led Mouginis-Mark *et al.* (1982) to suggest that mantle-forming Plinian eruptions occurred in the recent geologic past.

Some of the Elysium volcanoes, such as Hecates Tholus, have highly dissected flanks (Mouginis-Mark *et al.*, 1982, 1984; Gulick and Baker, 1990). It is also evident that the valley-forming events predate the eruption of the surrounding lava plains because the valleys are truncated by the plains (Figure 4.10). The dissection could reflect either erosion or volcanic flank deposits. Reimers and Komar (1979) proposed that lava or fast-moving pyroclastic flows may have carved the valleys. However, many of the valleys form midway on the flanks (Mouginis-Mark *et al.*, 1982) and have branches characteristic of surface runoff (Gulick and Baker, 1990). Local fluvial erosion could have resulted from hydrothermal release of water

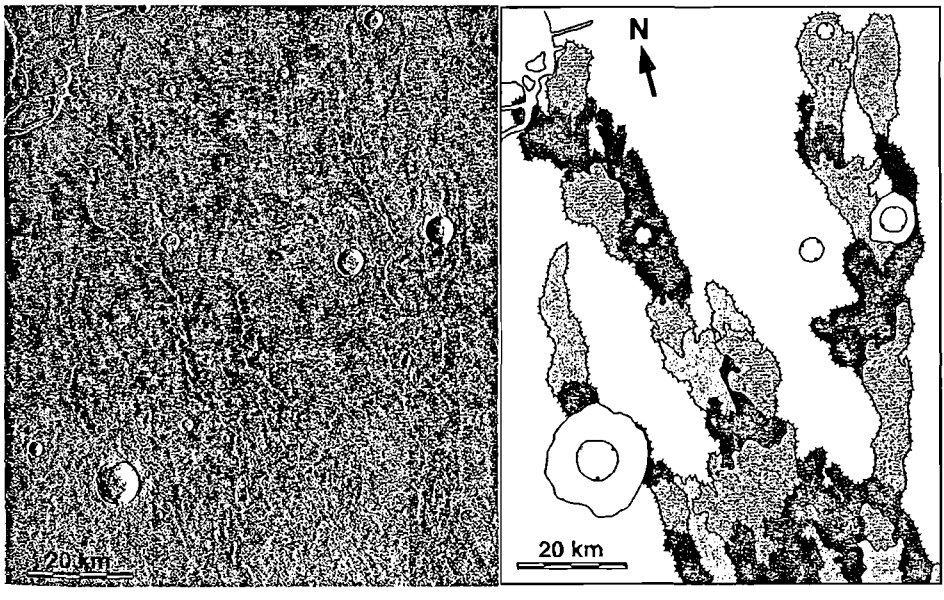

Figure 4.8. Left: View of segmented lava flows northwest of Elysium Mons. The distal ends of the flows are more than 300 km from the summit of Elysium Mons, and are estimated to be 40- to 60-m-thick flows (Mouginis-Mark and Tatsumura-Yoshioka, 1998). (Viking Orbiter frames 651A08–12.) Right: Geomorphic interpretation of the flows showing individual lobe segments; copyright, American Geophysical Union.

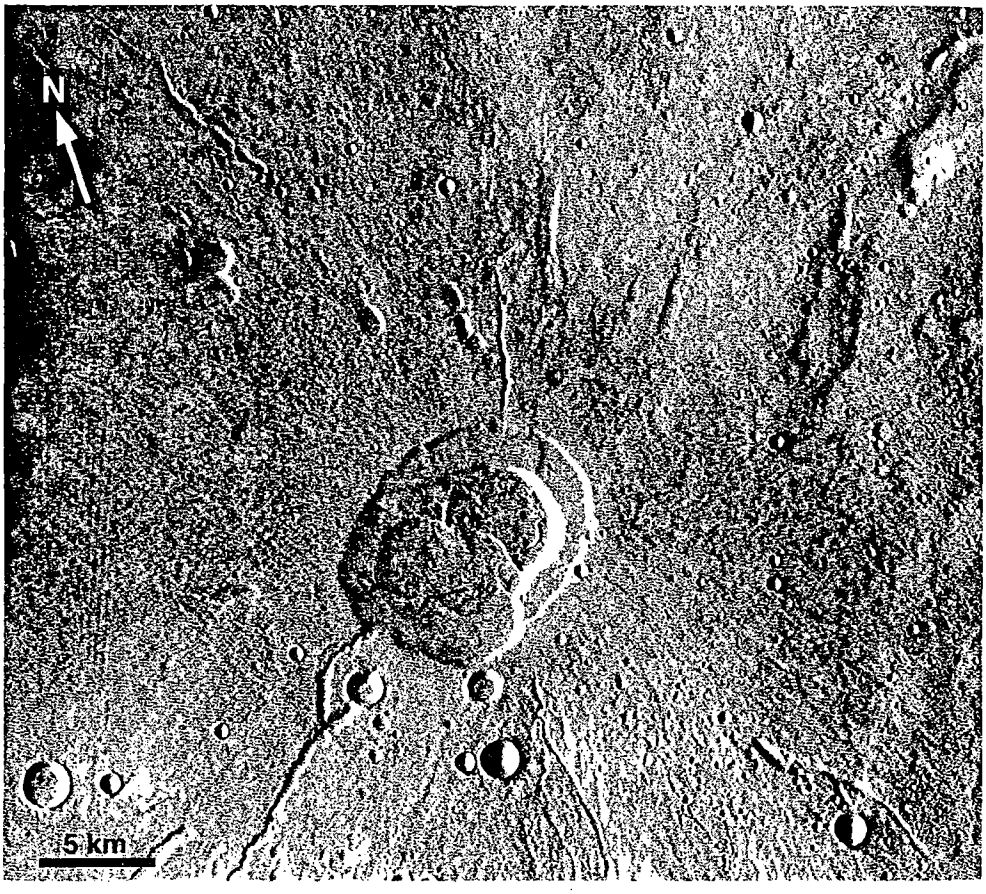

Figure 4.9. The summit area of Hecates Tholus has one of the best candidate ash fall deposits identified on Mars. The absence of small (<2 km) impact craters around the caldera suggests that a Plinian airfall deposit mantles the summit to a depth of ~100 m (Mouginis-Mark *et al.*, 1982). (Viking Orbiter frame 651A19.)

(Brackenridge *et al.*, 1985). The valleys show no evidence of lava flow fronts or other volcanic features (as found on the Tharsis volcanoes), and comparable valleys are found on the volcano Alba Patera. Therefore, Mouginis-Mark *et al.* (1988) proposed that the flanks are composed of easily eroded material, such as ash, and that the valleys formed by water-lubricated mass movements. In turn, this would imply that ash-producing eruptions occurred on Hecates Tholus, but not Elysium Mons, which lacks valleys.

4.5.3. Calderas

Calderas occur at the summits of all of the larger volcanoes on Mars. The calderas on the summits of Olympus Mons and Arsia Mons are representative of the morphologic range in Martian calderas (Crumpler *et al.*, 1996a). Variable distributions of strain at the surface are predicted in association with differences in shape, lateral dimensions, aspect ratio (width/height), and depth of individual magma chambers (Gudmundsson, 1988). An

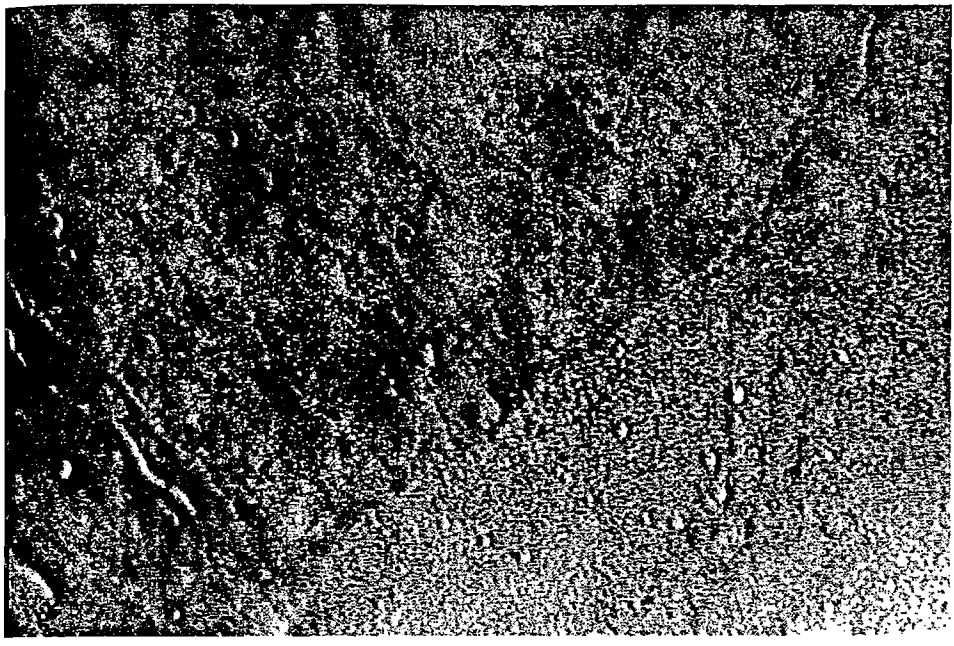

Figure 4.10. Narrow valleys in networks are found on the flanks of Hecates Tholus, Ceraunius Tholus, and Alba Patera. These valleys suggest that the flank materials are easy to erode, and could be ash deposits. The valleys shown here on the southeast flank of Hecates Tholus predate the emplacement of lava flows (lower right of figure) from Elysium Mons. (Viking Orbiter frame 651A22.)

additional factor in their morphologic diversity and larger dimensions may be the greater predicted depth and larger dimension of magma chambers on Mars relative to Earth (Wilson and Head, 1990).

The Olympus Mons caldera is irregular in planform, consisting of overlapping, nested, and scalloped margins with steep walls (Figure 4.11), and provides a record of the evolution of magma chamber size and location. The sequence in the complex is a trend from large calderas initially, followed by smaller local collapses (Mouginis-Mark and Robinson, 1992). However, the reverse trend is seen at Ascraeus Mons where the last caldera collapse formed a more circular and larger feature than previous calderas within the complex.

The Arsia Mons caldera is larger and more circular than typical terrestrial forms (Figure 4.11D). It has concentric fractures, ring grabens, and pit craters exterior to the caldera, and the walls are terraced. Topographic profiles (Smith *et al.*, 1998) show that the Arsia Mons caldera is relatively shallow and flat-floored. In contrast, the entire Pavonis Mons caldera complex appears to have sagged over a region 100 km across. Nested within the area is a single circular, steep-walled caldera 45 km across and as deep as 5 km.

The greater predicted depth and larger dimensions of magma chambers on Mars relative to Earth (Wilson and Head, 1990) are consistent with the larger dimensions of Martian calderas. Magma chambers form only if a zone of magma accumulation can develop (Wilson and Head, 1994) and if magma replenishment and thermal environment are sufficient for chamber growth (Crumpler *et al.*, 1996a). The necessary magma replenishment rate is controlled by the lithospheric thermal gradient and the shape and size of the magma chamber.

(A)

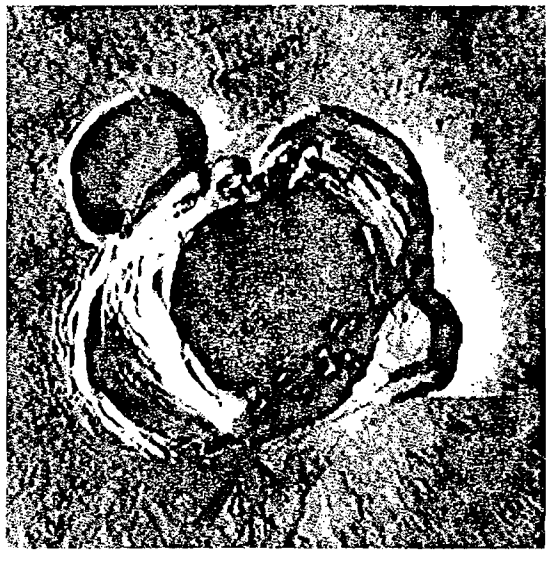

(B)

Figure 4.11. Martian calderas. (A) The summit caldera complex of Olympus Mons. Several smaller calderas are nested inside the larger, more circular caldera. (Viking Orbiter frame 890A68.). (B) The Ascraeus Mons caldera complex is similar to the Olympus Mons caldera, but has smaller calderas that overlap the margins of the largest caldera. (Viking Orbiter frames 892A 11,32).

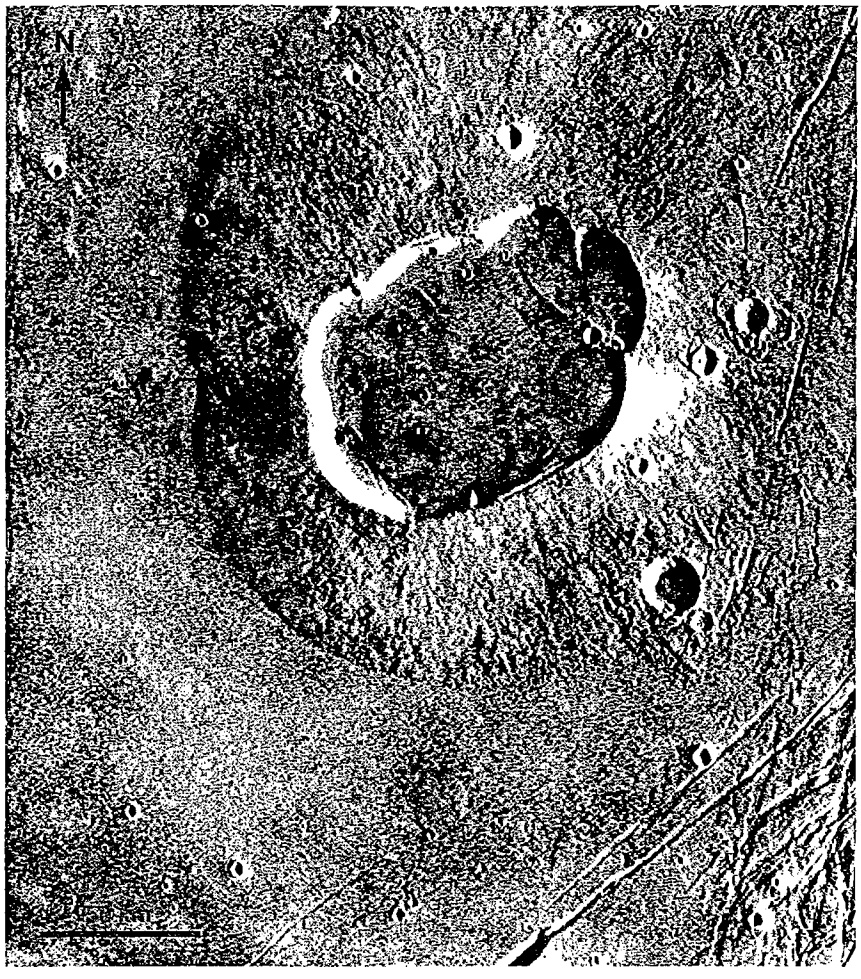

(C)

Figure 4.11. Martian calderas. (C) The Uranius Patera caldera is the result of the coalescence of several smaller calderas. (Viking Orbiter frames 857A43–46).

Crumpler *et al.* (1996b) suggest that the larger Martian calderas require replenishment rates that exceed Hawaiian rates.

4.5.4 Alba Patera

Alba Patera, north of the three Tharsis shield volcanoes, is unique on Mars (Carr *et al.*, 1977). It is larger in areal extent than Olympus Mons but lacks the relief of the shield volcanoes. It has flank slopes of $\sim 1°$ (Smith *et al.*, 1998) and is surrounded by a band of fractures suggesting that most flank flows were emplaced before the regional stress pattern was imposed. Impact crater densities indicate that Alba Patera is older than either the Tharsis or Elysium shield volcanoes (Neukum and Hiller, 1981). However, some young flows may represent eruptions that postdate the fractures (Schneeberger and Pieri, 1991). Materials

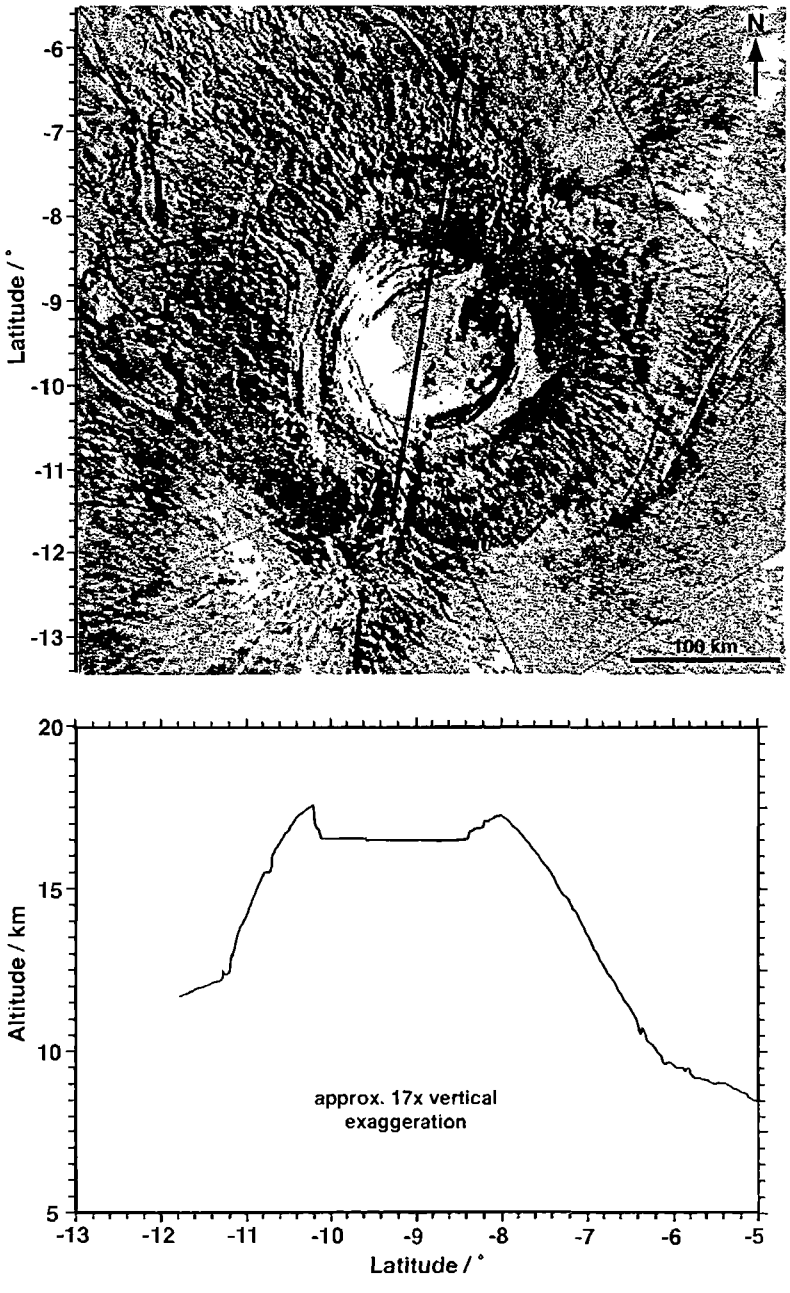

(D)

Figure 4.11. Martian calderas. (D) (Top) View of the circular caldera at the summit of the Arsia Mons shield volcano. The line represents the track of the MGS laser altimeter (MOLA; Smith *et al.*, 1998). (Part of Viking Orbiter mosaic MC-17NW.) (Bottom) MOLA topographic profile of Arsia caldera. The caldera is 123 km from rim to rim.

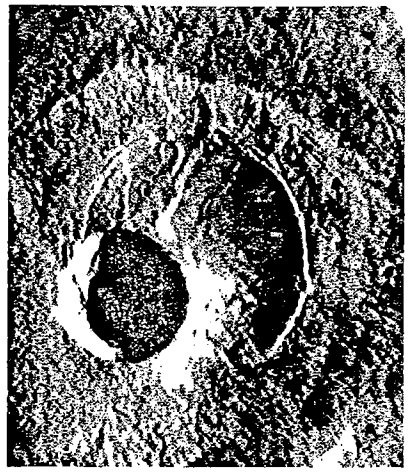

(E)

Figure 4.11. Martian calderas. (E) The summit caldera complex of Pavonis Mons (shown here) is similar to Arsia Mons in that there is a large circular subsidence, but is also similar to Olympus Mons in that there is a nested smaller caldera with terraced walls. (Viking Orbiter frame 643A54.)

surrounding the central zone could indicate both effusive and explosive volcanism (Mouginis-Mark *et al.*, 1988).

The western flanks of Alba Patera are composed of multiple tube- and channel-fed lava flows, many of which display partly collapsed lava tube segments. These flows were compared with similar features on Mt. Etna (Greeley and Spudis, 1981) and probably represent long-duration eruptions. Other flows are more sheetlike and lack channels and lava tubes. More detailed analyses of the Alba Patera flows are provided by Cattermole (1987). He also provides evidence for the existence of mild spatter and pyroclastic activity (Cattermole, 1986). Some flank areas have valley networks, suggesting fluvial erosion into pyroclastic deposits (Mouginis-Mark *et al.*, 1988). Alba Patera possesses two discrete calderas (Wood, 1984). The northernmost caldera is incomplete, and is filled on the eastern side by lava flows erupted from the southern caldera. This may indicate local topography or large-scale modifications to the magma plumbing system of the volcano during late-stage activity.

4.5.5. Discussion

Shield volcanoes on Mars display morphologies that are common on basaltic shields on Earth. Features typical of Martian volcanoes are large (>50 km) caldera complexes, which suggest that comparable-sized magma chambers were within 20 km of the volcano summits (Zuber and Mouginis-Mark, 1992).

Most of the youngest valley networks on Mars are found on volcanoes. This has been suggested as evidence against the idea that the early Martian climate was warm and wet and that it changed to the present cold and dry conditions (Carr and Chuang, 1997). For example, Hecates and Ceraunius Tholi lack well-preserved lava flows on their flanks but have valley networks that predate the emplacement of the surrounding plains lavas. The valleys could be fluvial features formed in unconsolidated pyroclastic deposits produced during explosive eruptions of the volcanoes. Alba Patera also has valley networks on its flanks, and may be

transitional in eruptive style between early explosive volcanism and more recent effusive activity on Mars (Mouginis-Mark *et al.*, 1988).

The environment may have played a role in the development of the basal units of several Martian volcanoes. Geomorphic evidence suggests that large bodies of water may have existed on Mars in the Amazonian Period (Baker *et al.*, 1991; Parker *et al.*, 1993). This is a controversial idea compared with the more generally accepted view of a "dry Mars" but it enables some of the features found with some volcanic landforms to be reinterpreted in a self-consistent manner. For example, the Olympus Mons escarpment is enigmatic. Early interpretations suggested erosion of cratered material on which the volcano was constructed (Head *et al.*, 1976) by the wind (King and Riehle, 1974). More recently, a tectonic origin was proposed for the scarp (Borgia *et al.*, 1990). Apollinaris Patera and Hecates Tholus also have a scarp, although lower in height (0.5–1.5 km) and smaller (Robinson *et al.*, 1993) than the Olympus Mons scarp. All three volcanoes have the lowest base elevations (<2 km above mean Mars datum) of Martian volcanoes and are adjacent to the putative shoreline of the hypothesized Martian seas (Baker *et al.*, 1991), so the basal scarps could be wave-cut features.

Considerable debate has also focused on the formation of the Olympus Mons aureole deposits. A central issue is the long size of the lobes. Ideas for the formation of the aureole include gravity spreading (Francis and Wadge, 1983; Tanaka, 1985), thrust faults and landslides (Harris, 1977; Lopes *et al.*, 1982), emplacement as ash flows (Morris, 1982), and subglacial lava flows (Hodges and Moore, 1979). Each mechanism requires low shear strength of the materials to facilitate sliding, and no equivalent runout slides have been identified on Earth. The closest analogies (Tanaka, 1985) are Hawaiian submarine landslides (Moore *et al.*, 1989). The Olympus Mons aureole deposits occur at low elevations (<1 km above Mars datum). In the model for shallow seas on Mars (Baker *et al.*, 1991), the entire northwest side of Olympus Mons would have been submerged, facilitating the formation of submarine slides, suggesting that they could be generated by the collapse of the submerged basal materials of the volcano.

Collapse of other Martian volcanoes might also be explained by the presence of unconsolidated basal materials. Tharsis Tholus (Figure 4.7) is relatively small and its summit is dissected by multiple sets of arcuate scarps (Robinson and Rowland, 1994). The scarps appear to represent a complex form of sector collapse comparable to that seen on volcanoes in Hawaii and Réunion Island (McGuire, 1996; Crumpler *et al.*, 1996b). Although the lower flanks of Tharsis Tholus are buried by younger flows, remnants of the edifice can be found to the northeast of the volcano, suggesting that the segments of the flanks have moved horizontally. By analogy with the terrestrial examples, it is possible that the basal unit of Tharsis Tholus is structurally weak, perhaps similar to the base of Olympus Mons (Mouginis-Mark, 1993).

4.6. MARTIAN HIGHLAND PATERAE

Highland paterae are low-relief, areally extensive central-vent volcanoes found in ancient cratered terrains on Mars, and are thought to be the oldest central-vent volcanoes on the planet (Plescia and Saunders, 1979). They are characterized by low shield morphology, central caldera complexes, and radial channels and ridges. The largest, best-imaged, and most extensively studied highland paterae are found around the Hellas basin.

Previous analyses of highland paterae include initial studies of Martian volcanoes based on Mariner 9 images, geologic mapping, surveys of volcanic features using Viking Orbiter images, and process-oriented studies. In addition, particular focus was placed on channels characteristic of patera flanks which may provide information on the environment in which the eruptions occurred.

Interpretations of the style(s) of eruption associated with highland paterae have changed with time. Mariner 9 data suggested that Amphitrites, Hadriaca, and Tyrrhena Paterae were basaltic shield volcanoes, formed from low-viscosity lavas (Potter, 1976; Peterson, 1977, 1978; King, 1978). Their formation by pyroclastic eruptions was thought improbable because the extensive erosion expected in ancient pyroclastic deposits was not observed in Mariner 9 images (Peterson, 1978).

Viking Orbiter images resulted in reevaluation of patera origins (Carr, 1981). The geomorphology of Tyrrhena Patera and its erosional characteristics led Greeley and Spudis (1981) to propose that phreatomagmatic activity, caused by magma rising through water-rich megaregolith, was the dominant eruptive mechanism. Francis and Wood (1982) suggested that the highland paterae could be mafic pyroclastic structures with eruptions driven by volatiles from sources at great depths. They argued that large-scale, evolved magmatic activity was improbable and that phreatomagmatic activity at a scale large enough to produce the paterae was unlikely, based on terrestrial analogues. Later examinations of Tyrrhena and Hadriaca Paterae, including geomorphic analyses and corresponding assessments of eruption mechanisms, suggest that they consist of pyroclastic flow deposits. An evaluation of the energy required to emplace the patera flank materials indicates that eruptions driven by either magmatic volatiles or ground water are viable (Greeley and Crown, 1990; Crown and Greeley, 1993).

4.6.1. Tyrrhena Patera

The flanks of Tyrrhena Patera consist of layered, friable deposits dissected by extensive erosional channels radial to the summit region (Figure 4.12). The ~50-km caldera complex includes ring fractures and two connected depressions. A large channel extends from the depressions to the southwest where it joins a flank flow unit ~1000 km long (Greeley and Crown, 1990). The flank flow may have been supplied by this channel and contains numerous ~100-km-long lava flows and parts of a leveed channel system that may have spanned ~600 km. These lava flows are the only clear evidence of effusive volcanic activity. Based on crater statistics, the flows were emplaced in the Late Hesperian/Early Amazonian Epochs, long after the earlier shield-building materials (Crown *et al.*, 1992; Gregg *et al.*, 1998). Viking Orbiter images with resolutions as high as ~10 m pixel^{-1} show no evidence of primary flow features within the flank deposits, which exhibit erosional surfaces at the limits of resolution (Crown and Greeley, 1993).

4.6.2 Hadriaca Patera

The summit of Hadriaca Patera (Figure 4.13) is marked by a well-defined, nearly circular caldera ~77 km across. The caldera appears to be filled with late-stage lavas. A large, curvilinear wrinkle ridge and small domelike features in the eastern part of the caldera, together with the scalloped rim suggest a complex history. The flanks of the volcano are asymmetric in plan view (~300 × 560 km) and exhibit layering and remnant mesas. The flank channels are trough-shaped, lack tributaries, and are continuous over long distances.

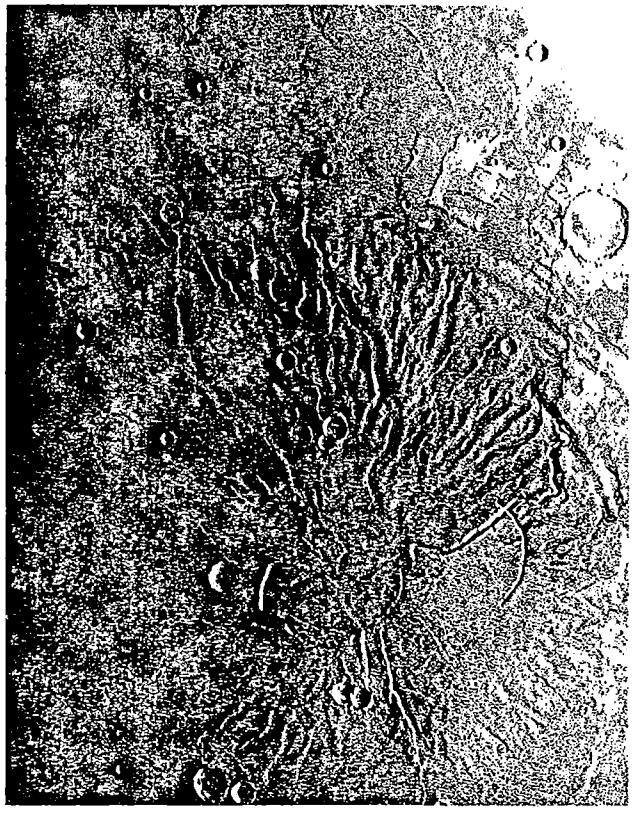

(A)

Figure 4.12. Volcano flanks. (A) View of Tyrrhena Patera showing the complex summit region surrounded by its eroded flanks. A large rille extends to the southwest and connects the caldera complex to the flank flow unit consisting of numerous lava flow lobes. The summit caldera complex is ~50 km across. North is to the upper right corner of the image. (Viking Orbiter frame 087A14.)

Amphitheater-headed channels are common. The erosional morphology of the channeled flanks of Hadriaca and Tyrrhena Paterae is attributed to a combination of ground water sapping and surface runoff, with more extensive surface dissection evident at Hadriaca Patera in the form of V-shaped valley interiors (Gulick and Baker, 1990; Crown and Greeley, 1993). Crater statistics suggest that Hadriaca Patera formed in the Early Hesperian Epoch and has a slightly younger surface than Tyrrhena Patera (Crown *et al.*, 1992).

4.6.3. Amphitrites/Peneus Patera Complex

The Amphitrites/Peneus Patera complex is defined by two large (~120 km in diameter) circular depressions and surrounding dissected and ridged plains. Amphitrites Patera exhibits nested, shallow depressions that are surrounded by a distinctive radial channel system similar to those at Tyrrhena and Hadriaca Paterae. Peneus Patera consists of concentric fractures surrounded and flooded by ridged plains. The degradation of small impact craters in the

(B)

Figure 4.12. Volcano flanks. (B) The eroded flanks of Tyrrhena Patera show nested channels indicative of headward erosion. Lineations potentially related to wind erosion are observed orthogonal to the channel orientation. The frame is ~15 km across. North is to the bottom left corner. (Viking Orbiter image 794A01.)

region suggests a complex and extensive history of modification. The Amphitrites/Peneus Patera complex was initially interpreted as an overlapping complex of low shield volcanoes (Potter, 1976; Peterson, 1977, 1978) with up to six source calderas. This complex could be the source of the ridged plains of Malea Planum (Greeley and Guest, 1987; Tanaka and Scott, 1987).

4.6.4 Tempe Patera

Tempe Patera is found in the northern hemisphere. It consists of a shallow, 16-km-diameter depression surrounded by smooth deposits that are extensively degraded by radial, poorly defined shallow troughs (Plescia and Saunders, 1979; Wise, 1979; Hodges and Moore, 1994). Its morphology is generally similar to that of Tyrrhena Patera, although it is much smaller. Plescia and Saunders (1979) indicate that Tempe Patera is as old as, or slightly older than, Tyrrhena Patera. A potentially similar feature ~100 km across found in the Thaumasia region was interpreted to be a volcano by Scott and Tanaka (1981) and Scott (1982) but does not have the distinct central vent characteristics of other highland paterae.

(C)

Figure 4.12. Volcano flanks. (C) View of a lava flow lobe within the flank flow southwest of the Tyrrhena Patera summit. The upper, more irregular part of the flow lobe has a channel in its interior that appears to have fed a wider, ~60-km-long unchannelized zone. North is to the top of the image. (Part of Viking Orbiter image 413S13.)

4.6.5. Summary

The geologic evolution and styles of eruptive activity for the Martian highland paterae have significant implications for interpreting the volcanic and climatic history of Mars. Highland paterae are the oldest preserved central-vent volcanoes on Mars and could represent a transition from earlier plains-forming volcanic activity to large discrete eruptive centers (Greeley and Spudis, 1981). In addition, most paterae represent basin-related, highland volcanic centers that provide a basis for comparison with Martian shields and tholi, and they may provide evidence for differences in magma source regions between the highlands and the northern lowlands and/or temporal changes in Martian magmas or their emplacement conditions (Crown and Greeley, 1993).

Use of the paterae in comparisons with other volcanoes or for inferences about the environment depends on interpretations of their eruptive style. The interpretation of phreatomagmatic activity for Tyrrhena and Hadriaca Paterae is consistent with the timing and extent of aqueous erosion documented for the region. The lack of volcanoes with morphologic characteristics similar to highland paterae in younger volcanic provinces and the

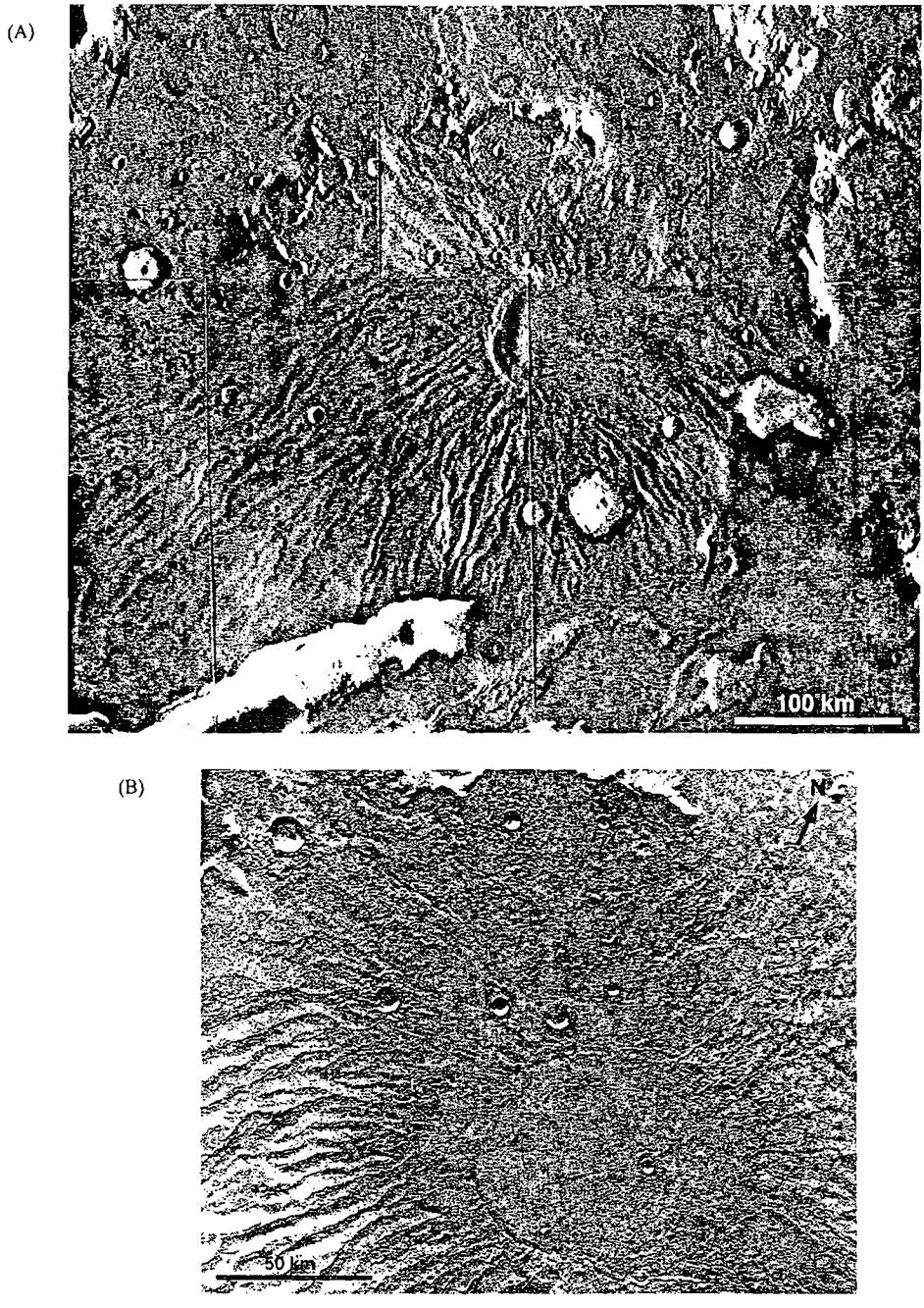

Figure 4.13. Hadriaca Patera. (A) View of the summit caldera (~77 in diameter) and surrounding channeled flanks of Hadriaca Patera. Collapse features associated with Dao Vallis are observed to the east (right) and south (bottom) of Hadriaca Patera and truncate its flanks. North is to the upper right corner of the image. (Part of Viking Orbiter photo-mosaic 211-5456.) (B) Detailed view of the summit of Hadriaca Patera. The western rim (left) of the caldera suggests multiple episodes of collapse, whereas the rim to the north and east may be covered by eruptive products. A large scarp in the southeast may be the margin of lava ponded in the caldera; small domelike features are observed on the surface of caldera-filling materials to the east. North is to the upper right corner of the image. (Viking Orbiter image 410S02.)

inferred transition from explosive to effusive volcanism at Tyrrhena and Hadriaca Paterae may reflect a global change in Martian near-surface and atmospheric conditions that limited or depleted the volatiles necessary to generate hydrovolcanic eruptions.

If magmatic volatiles drove explosive eruptions at the highland paterae, the generation of less volatile-rich magmas over time could explain the transitions thought to occur in the eastern Hellas region, as well as the observed difference in volcano morphology between the highlands and the Tharsis and Elysium provinces (Francis and Wood, 1982; Crown and Greeley, 1993). Heterogeneities in magma source regions may also be a factor. If the early suggestions that the paterae consist of fluid lavas prove to be true, lava flows associated with the paterae could indicate significantly different thermal environments, magma bodies, emplacement conditions, or erosional regimes than are typical of the younger volcanoes on the Martian surface.

4.7. SMALL VOLCANIC CONSTRUCTS

Clusters of kilometer-sized conical hills, many with summit craters, are found in the northern plains and southern highlands. Fields of knobs, buttes and eroded hills in the Aeolis (Greeley and Spudis, 1981), Thaumasia (Scott, 1982), and Tempe (Plescia and Saunders, 1979) regions are suggested to be volcanoes. In each case, image resolution and erosion of the features make their origin unclear. For example, the thousands of small hills in Acidalia and Utopia Planitiae (Frey and Jarosewich, 1982) could be cinder cones, but they could equally well be pingos or volcanic pseudocraters formed from lava flows.

Martian surface conditions might also complicate recognition of small volcanoes in low-resolution images. For example, the lower Martian gravity could cause pyroclastic eruptions to spread cinders over a wider area than for similar eruptions on Earth. At least some of the "lava shields" in Tempe Terra (Plescia, 1981) could have formed in this manner. The small hills aligned across the floor of Arsia Mons caldera (Carr *et al.*, 1977) may also be cinder cones. Small ridges on Alba Patera were interpreted as spatter ridges produced by low-level fire-fountaining (Cattermole, 1986), but diagnostic features are too small to be seen on available data.

With evidence for volcanism and ground ice in close proximity (Allen, 1979; Hodges and Moore, 1979; Mouginis-Mark, 1985; Squyres *et al.*, 1987), it is unclear why more maars have not been identified. One possibility is that the resultant craters would be morphologically similar to small impact craters and have been misinterpreted. As with cinder cones, the low Martian gravity would cause greater ejecta dispersal, leading to low, wide crater rims. High-resolution images could shed light on volcano/ground ice interactions, as well as other aspects of Martian volcanic features.

4.8. VOLCANIC PLAINS

Volcanic plains of several types are found on Mars. The most widespread are ridged plains that resemble the lunar maria. They are characterized by wrinkle ridges and commonly fill older impact craters, but rarely display vents or vent structures. As with the lunar maria, the ridged plains on Mars are thought to represent flood lavas erupted at high rates of effusion from fissures that were buried by their own products. Lack of distinctive flow features such as lobes and flow fronts suggests that the lavas were extremely fluid, perhaps comparable to

komatiites erupted on Earth in the Precambrian. The lack of flow features, however, also means that their interpretation as volcanic is uncertain.

Some plains areas, as shown in Figure 4.3, are clearly volcanic, as evidenced by distinct flow lobes, and constitute a second type of volcanic plains. They form widespread sheets and typically lack lava channels and apparent lava tubes at the resolution of Viking images. As with the ridged plains, these flows could have been emplaced from massive eruptions; however, the lavas might not have been as fluid, but rather possessed greater viscosities, resulting in preservation of flow margins and fronts.

A third type of volcanic plains is associated with some of the large constructs. For example, lava flows can be traced from the flanks of Olympus Mons and onto the surrounding plains. These units also have distinctive flow fronts and side lobes. Together with ridged plains and the sheet flows described above, these constitute plains of *probable* volcanic origin.

Martian plains of *possible* volcanic origin are found throughout much of the northern lowlands. Flow lobes and ventlike structures are seen in high-resolution images in some areas. However, imaging resolution and quality are insufficient to map most of the lowland plains consistently; these plains probably are composed of materials of many diverse origins, including volcanic.

Plains of probable volcanic origin constitute more of the Martian surface than any other terrain (Greeley and Spudis, 1981; Greeley and Schneid, 1991). Although they appear to have attained their greatest areal extent in the early Hesperian (Tanaka *et al.*, 1988; Greeley and Schneid, 1919), this is likely to be an artifact of preservation. For example, all of the northern lowlands are of probable volcanic origin but subsequent burial and reworking with sediments may have obscured their volcanic origin. Moreover, the likely thermal history of Mars suggests extensive volcanism in the Noachian Period but intense impact cratering has destroyed this record. The morphologies of small areas of Noachian age in the highlands (chiefly in the Arabia to Noachis Terra regions; Figure 4.14) are consistent with lava plains emplacement.

Ridged plains that could be comprised of lava flows are abundant around many volcanic centers, such as Hesperia Planum in the vicinity of Tyrrhena Patera (Figure 4.15). In addition, lobate flows associated with volcanic centers, and channels similar to lunar sinuous rilles are evidence for volcanic plains surrounding volcanic centers in some highland settings.

Extensive Hesperian volcanic plains were emplaced as precursors to the Tharsis and Elysium volcanic regions. The intravolcano plains in the Tharsis area were further surfaced by lobate and digitate lava flows, many of which represent late-stage eruptions (Figures 4.11, 4.16 and 4.17).

Morphologies of some lava plains flows might have been affected by local variations in the Martian environment. Mouginis-Mark and Tatsumura-Yoshioka (1998) mapped the area north and west of Elysium Mons, where 59 large lava flows were identified. Some of these flows can be divided into discrete segments that could represent emplacement as a series of pulses (Figure 4.8). Each breakout of a new flow segment appears to have occurred at the distal end of the earlier lobe. Lengths range from 9 to 41 km and maximum thicknesses range from 40 to 125 m. The surface of each flow is flat, lacks festoon ridges, and is interpreted to be a'a (Bruno *et al.*, 1992). There is no evidence for lava tubes, roofed channels, or lobes emerging from the sides of earlier lobes, so that some (unknown) limit imposed by properties of the flow prevented their lateral growth. The relatively flat surfaces suggest that flow inflation was not part of the emplacement. Similar flow segmentation was described by Gregg and Fink (1997) in laboratory simulations under conditions that they call the rifting regime; the simulated lava temporarily had a sufficient hydraulic pressure to rupture the crust.

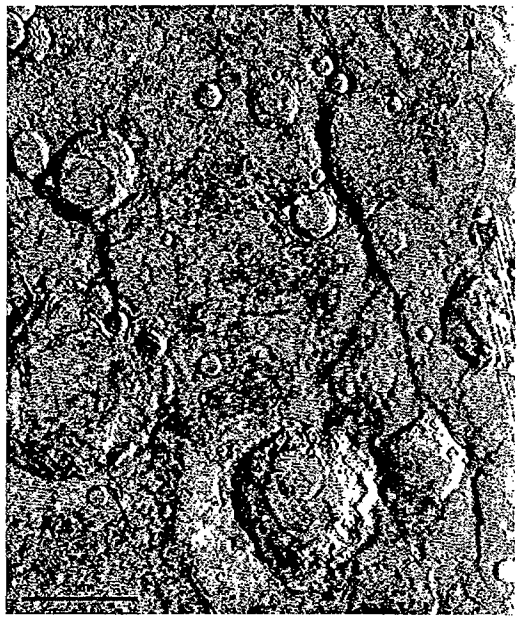

Figure 4.14. Possible volcanic plains of Noachian age, showing the "flooded" appearance of impact craters and mare-type wrinkle ridges typical of volcanic plains on the Moon. Image is 22 km wide, centered at 33°N latitude, 306.5°W longitude. (Viking Orbiter frames 641A14, 16–18.)

Another type of segmented flow occurs northwest of the Alba Patera caldera. Called "M-type flows" by Lopes and Kilburn (1990), they appear to be topographically constrained, so that individual flows might have been forced by adjacent high points to override earlier flow lobes. However, image resolution for these flows is ~80 m pixel^{-1} and direct comparison with those in the Elysium Planitia field is not possible. Although Viking Orbiter image resolution varies over the planet, it appears that segmented lava flows are rare on Mars and they could indicate unusual eruptions and/or emplacement conditions. For example, the flat preflow terrain, abundant permafrost, or pulsing of the flow could have produced the segmented flows (Mouginis-Mark and Tatsumura-Yoshioka, 1998). Other morphologic evidence also suggests that northwest Elysium Planitia has been affected by subsurface volatiles. Many of the graben have outflow deposits suggestive of surface water flow (Mouginis-Mark, 1985) and an area of chaos just north of the lava flows appears to have formed by collapse following the removal of ground ice (Carr and Schaber, 1977), perhaps leading to lahar deposition (Christiansen and Greeley, 1981; Christiansen, 1989). Alternately, this area has been interpreted as glacial outflow deposits associated with subice eruptions (see Chapter 3).

4.9. CONCLUSION

Despite more than three decades of exploration by spacecraft, many fundamental questions regarding Martian volcanism remain unanswered. The following is not a complete

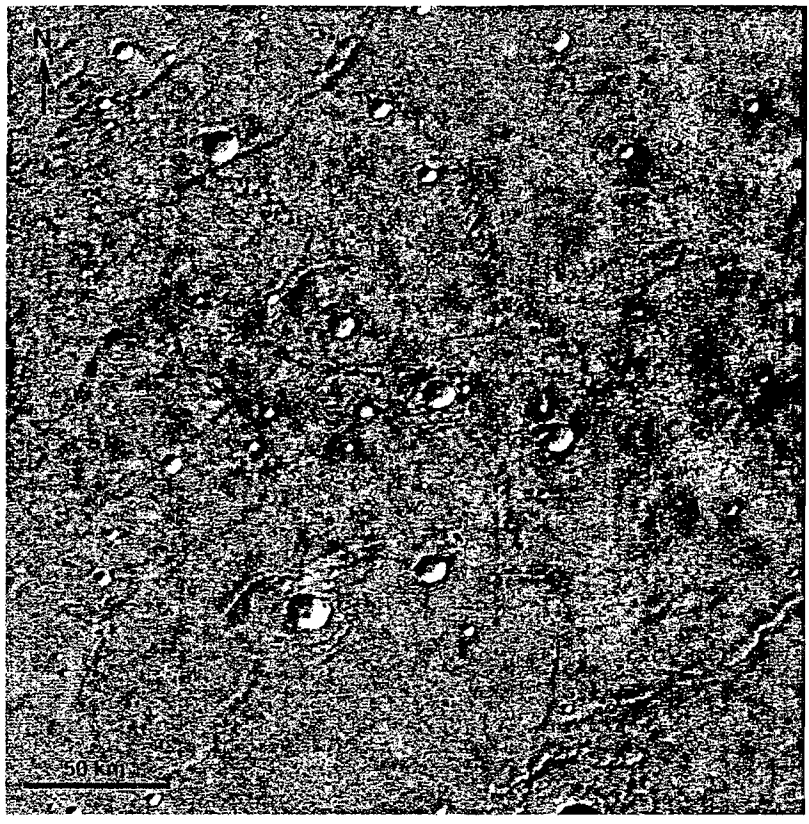

Figure 4.15. Hesperian-age ridged plains east of Tyrrhena Patera. Plains of similar morphology are among the most extensive probable volcanic areas on Mars. Image is 270 km wide, centered at 21.5°S latitude, 249°W longitude. (Viking Orbiter frames 391S51, 87A14–17.)

compilation, but includes some of the issues regarding the role of the Martian environment in controlling the styles of volcanism and the resulting volcanic features:

1. Do the changes in volcanic morphology and inferred styles of volcanism for the highland paterae reflect a change in Martian environment in which surface or near-surface volatiles were depleted (Greeley and Spudis, 1981), or do the changes represent magma evolution or other factors? How has the atmospheric pressure/density changed over time, and how would this affect eruptive styles and volcanic morphology?
2. Do the channels on some of the volcanoes, such as Hecates Tholus (Mouginis-Mark *et al.*, 1982), represent local climatic regimes that allowed precipitation; alternatively, could the channels represent a form of volcanism or flow emplacement not previously recognized?
3. Do the wrinkle ridges represent deformation of volcanic materials, or are they structural features that can form in rock units of any type? As discussed by Greeley and Spudis (1981), mare-type ridges are commonly used to infer marelike basalts on planetary surfaces by lunar analogy, but the criterion of the presence of such ridges is far from definitive.

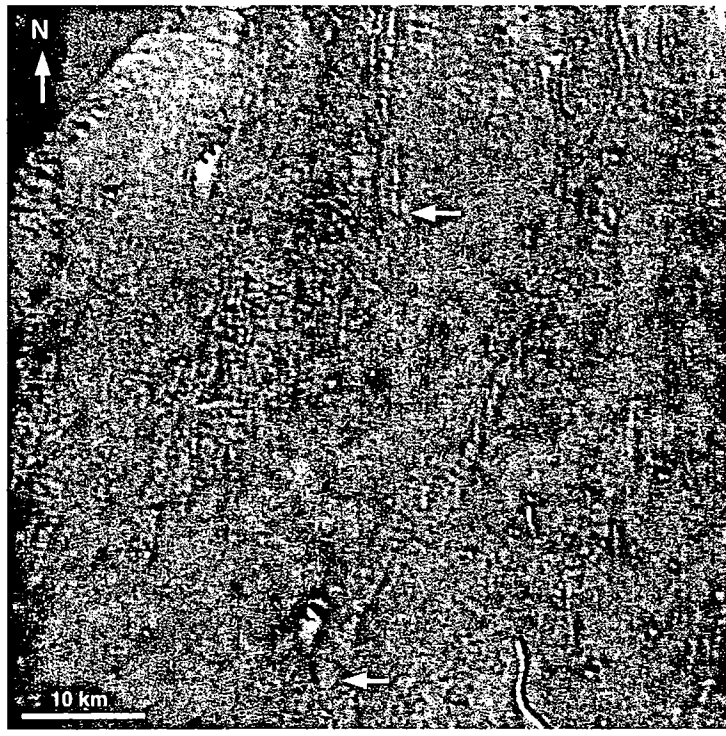

Figure 4.16. Amazonian-age volcanic plains in the Tharsis region of Mars south of Arsia Mons. Lobate fronts of individual digitate lava flows are indicated by arrows. Image is 60 km wide, centered at 17°S latitude, 115°W longitude. (Viking Orbiter frame 56A28.)

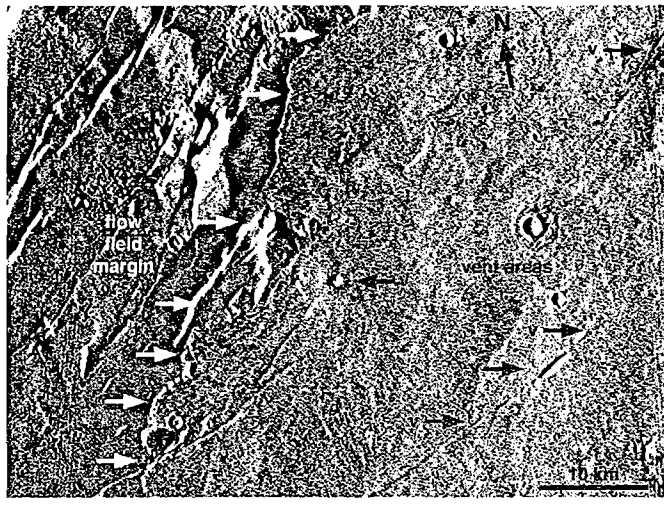

Figure 4.17. Volcanic centers and surrounding lava plains in the Tempe–Mareotis region of Mars. Similar plains occur in several areas surrounding the Tharsis region and appear to have formed by eruption of sheets of lava from numerous small vents (black arrows). (Viking Orbiter frame 627A27.)

4. When did the last eruptions occur on Mars? Although the SNC meteorites indicate that some eruptions may have occurred 120 Ma (McSween, 1994), the exact source of the SNCs on Mars is conjectural (Plescia, 1993) and they probably do not represent the latest eruptions. Mars Global Surveyor images will enable assignments of relative ages to flows and other volcanic features, but the absolute chronology will only be determined when samples are returned to Earth from specific volcanic areas.
5. What is the chemical diversity of lavas on Mars, and is there a correlation between volcano morphology and chemistry? Most investigators attribute differences among volcanic features to interaction of the magma with near-surface volatiles or other eruption parameters (Mouginis-Mark *et al.*, 1982; Crown and Greeley, 1993; Robinson *et al.*, 1993; Wilson and Head, 1994). Thermal Emission Spectrometer (Christensen *et al.*, 1992) data from Mars Global Surveyor, other remote sensing data, and measurements made by landers might resolve the issue of chemical diversity of Martian volcanic rocks.
6. What is the topography of Martian volcanoes and lava flows? The slope and thickness of individual flows are very poorly constrained and estimates of lava rheology (e.g., Zimbelman, 1985; Cattermole, 1987; Lopes and Kilburn, 1990; Glaze and Baloga, 1998) at the time of emplacement may be significantly in error. Similarly, the summit caldera volumes and edifice heights might also be in error, which has important implications for the volume of the magma chamber, the size of a caldera-forming event (Zuber and Mouginis-Mark, 1992), and the dynamics that initiated the eruption (Wilson and Head, 1994).

Some of these issues will be resolved with additional measurements and observations from current and ongoing missions, as outlined above. The international space exploration program has a focus on Mars in the late 1990s and well into the next century. Approved and planned missions have the potential to return a great wealth of data on the history of Mars and its evolution through time. Combined with missions that will return a series of samples from Mars, laboratory experiments, theoretical considerations, and study of relevant terrestrial analogues should ensure that the next decade sees a significant improvement in our understanding of Mars, its volcanic history, and the role of the environment in controlling volcanic processes.

ACKNOWLEDGMENTS

R. G. and S. A. F. were supported partly by the NASA Planetary Geology and Geophysics Program; J. R. Z. was supported partly by NASA grants NAGW-1390 and NAG5-4586. L. S. C. was supported by NASA grant NAG5-4309. D. A. C. was supported partly by NASA grants NAG5-4037 and NAG5-3642. We appreciate reviews provided by M. Chapman, J. A. Crisp, J. W. Head, and L. Wilson.

4.10. REFERENCES

Allen, C. C., Volcano–ice interactions on Mars, *J. Geophys. Res.*, *84*, 8048–8059, 1979.

Anderson, D. L., The internal composition of Mars, *J. Geophys. Res.*, *77*, 789–795, 1972.

Baker, V. R., G. Komatsu, R. G. Strom, V. C. Gulick, J. S. Kargel, and V. S. Kale, Ancient oceans, ice sheets, and the hydrologic cycle of Mars, *Nature*, *352*, 589–594, 1991.

Banin, A., B. C. Clark, and H. Wänke, Surface chemistry and mineralogy, in *Mars*, edited by H. H. Kieffer, B. M. Jakosky, C. W. Snyder, and M. S. Matthews, pp. 594–625, University of Arizona Press, Tucson, 1992.

Bell, J. F., Iron, sulfate, carbonate, and hydrated minerals on Mars, in *Mineral Spectroscopy: A Tribute to Roger G. Burns, Geochemical Society Special Publication 5*, edited by M. D. Dyar, C. McCammon, and M. W. Schaefer, pp. 359–380, 1996.

Blaney, D. L., and T. B. McCord, An observational search for carbonates on Mars, *J. Geophys. Res.*, *95*, 10159–10166, 1990.

Blaney, D. L., and T. B. McCord, Indications of sulfate minerals in the Martian soil from Earth-based spectroscopy, *J. Geophys. Res.*, *100*, 14433–14441, 1995.

Blasius, K. R., and J. A. Cutts, Topography of Martian central volcanoes, *Icarus*, *45*, 87–112, 1981.

Borgia, A., J. Burr, W. Montero, L. D. Morales, and G. E. Alvarado, Fault propagation folds induced by gravitational failure and slumping of the central Costa Rica volcanic range: Implications for large terrestrial and Martian volcanic edifices, *J. Geophys. Res.*, *95*, 14357–14382, 1990.

Brackenridge, G. R., H. E. Newsom, and V. R. Baker, Ancient hot springs on Mars: Origins and paleoenvironmental significance of small Martian valleys, *Geology*, *13*, 859–862, 1985.

Bridges, N. T., R. C. Anderson, J. A. Crisp, T. Economou, and R. Reid, Separating dust and rock APXS measurements based on multispectral data at the Pathfinder landing site, *EOS (Trans. Am. Geophys. Union)*, *78*, F402–F403, 1997.

Bruno, B. C., G. J. Taylor, S. K. Rowland, P. G. Lucey, and S. Self, Lava flows are fractals, *Geophys. Res. Lett.*, *19*, 305–308, 1992.

BVTP, *Basaltic Volcanism on the Terrestrial Planets*, Pergamon Press, New York, 1981.

Carr, M. H., Volcanism on Mars, *J. Geophys. Res.*, *78*, 4049–4062, 1973.

Carr, M. H., *The Surface of Mars*, 232 pp, Yale University Press, New Haven, 1981.

Carr, M. H., *Water on Mars*, 229 pp., Oxford University Press, London, 1996.

Carr, M. H., and F. C. Chuang, Martian drainage densities, *J. Geophys. Res.*, *102*, 9145–9152, 1997.

Carr, M. H., and R. Greeley, *Volcanic Features of Hawaii: A Basis for Comparison with Mars*, NASA SP-403, 211 pp., 1980.

Carr, M. H., and G. G. Schaber, Martian permafrost features, *J. Geophys. Res.*, *82*, 4039–4065, 1977.

Carr, M. H., and H. Wanke, Earth and Mars: Water inventories as clues to accretional histories, *Icarus*, *98*, 61–71, 1992.

Carr, M. H., R. Greeley, K. R. Blasius, J. E. Guest, and J. B. Murray, Some Martian volcanic features as viewed from the Viking orbiters, *J. Geophys. Res.*, *82*, 3985–4015, 1977.

Cattermole, P., Linear volcanic features at Alba Patera–Probable spatter ridges, *J. Geophys. Res.*, *91*, E159–E165, 1986.

Cattermole, P., Sequence, rheological properties, and effusion rates of volcanic flows at Alba Patera, Mars, *J. Geophys. Res.*, *92*, E553–E560, 1987.

Christensen, P. R., D. L. Anderson, S. C. Chase, R. N. Clark, H. H. Kieffer, M. C. Malin, J. C. Pearl, J. Carpenter, N. Bandiera, F. G. Brown, and S. Silverman, Thermal Emission Spectrometer Experiment: Mars Observer mission, *J. Geophys. Res.*, *97*, 7719–7734, 1992.

Christensen, P. R., D. L. Anderson, S. C. Chase, R. T. Blancy, R. N. Clark, B. J. Conrath, H. H. Kieffer, R. O. Kuzmin, M. C. Malin, J. C. Pearl, T. L. Roush, and M. D. Smith, Results from the Mars Global Surveyor Thermal Emission Spectrometer, *Science*, *279*, 1692–1698, 1998.

Christiansen, E. H., Lahars in the Elysium region of Mars, *Geology*, *17*, 203–206, 1989.

Christiansen, E. H., and R. Greeley, Megalahars(?) in the Elysium region, Mars, *Lunar Planet. Sci.*, *12*, 138–140, 1981.

Clemens, J. D., Water contents of silicic to intermediate magmas, *Lithos*, *17*, 273–287, 1984.

Clifford, S. M., A model for the hydrologic and climatic behavior of water on Mars, *J. Geophys. Res.*, *98*, 10973–11016, 1993.

Crown, D. A., and R. Greeley, Volcanic geology of Hadriaca Patera and the eastern Hellas region of Mars, *J. Geophys. Res.*, *98*, 3431–3451, 1993.

Crown, D. A., K. H. Price, and R. Greeley, Geologic evolution of the east rim of the Hellas basin, Mars, *Icarus*, *100*, 1–25, 1992.

Crumpler, L. S., J. W. Head, and J. C. Aubele, Magma chambers associated with calderas on Mars: Significance of long-term magma replenishment rates, *Lunar Planet. Sci.*, *26*, 305–306, 1996a.

Crumpler, L. S., J. W. Head, and J. C. Aubele, Calderas on Mars: Characteristics, structural evolution, and associated flank structures, in *Volcanic Instability on Earth and Other Planets*, Geological Society of London Special Publication, *110*, 307–347, 1996b.

Dreibus, G., and H. Wanke, Mars, a volatile-rich planet, *Meteoritics*, *20*, 367–381, 1985.

Dreibus, G., E. Jagoutz, and H. Wanke, Water in the Earth's mantle, *Geol. Geofiz.*, *38*, 269–275, 1997.

Edgett, K. S., Possible cinder cones near the summit of Pavonis Mons, Mars, *Lunar Planet. Sci. Conf.*, *21*, 311–312, 1990.

Edgett, K. S., Aeolian dunes as evidence for explosive volcanism in the Tharsis region of Mars, *Icarus*, *130*, 96–114, 1997.

Edgett, K. S., B. J. Butler, and J. R. Zimbelman, Geologic context of the Mars radar "Stealth" region in southwestern Tharsis, *J. Geophys. Res.*, *102*, 21545–21567, 1997.

Fagents, S. A., and L. Wilson, Numerical modeling of ejecta dispersal around the sites of volcanic explosions on multiple regression, *Icarus*, *123*, 284–295, 1996.

Fink, J. H., Surface folding and viscosity of rhyolite flows, *Geology*, *8*, 250–254, 1980.

Folkner, W. M., C. F. Yoder, D. N. Yuan, E. M. Standish, and R. A. Preston, Interior structure and seasonal mass redistribution of Mars from radio tracking of Mars Pathfinder, *Science*, *278*, 1749–1752, 1997.

Francis, P. W., and G. Wadge, The Olympus Mons aureole: Formation by gravitational spreading, *J. Geophys. Res.*, *88*, 8333–8344, 1983.

Francis, P. W., and C. A. Wood, Absence of silicic volcanism on Mars: Implications for crustal composition and volatile abundance, *J. Geophys. Res.*, *87*, 9881–9889, 1982.

Frey, H., and M. Jarosewich, Subkilometer Martian volcanoes: Properties and possible terrestrial analogs, *J. Geophys. Res.*, *87*, 9867–9879, 1982.

Frey, H., B. L. Lowry, and S. A. Chase, Pseudocraters on Mars, *J. Geophys. Res.*, *84*, 8075–8086, 1979.

Gill, J., *Orogenic Andesites and Plate Tectonics*, 390 pp., Springer-Verlag, Berlin, 1981.

Glaze, L. S., and S. M. Baloga, Dimensions of Puu Oo lava flows on Mars, *J. Geophys. Res.*, *103*, 13659–13666, 1998.

Greeley, R., Mariner 9 photographs of small volcanic structures on Mars, *Geol. Soc. Am.*, *1*, 175–180, 1973.

Greeley, R., Volcanic morphology, in *Volcanism of the Eastern Snake River Plain, Idaho: A Comparative Planetary Geology Guidebook*, NASA CR-154621, 1977.

Greeley, R., and D. A. Crown, Volcanic geology of Tyrrhena Patera, Mars, *J. Geophys. Res.*, *95*, 7133–7149, 1990.

Greeley, R., and J. E. Guest, Geologic map of the eastern equatorial region of Mars, *U.S. Geol. Surv. Misc. Invest. Ser. Map, I-1802B*, 1987.

Greeley, R., and P. D. Spudis, Volcanism in the cratered terrain hemisphere of Mars, *J. Geophys. Res.*, *5*, 453–455, 1978.

Greeley, R., and P. D. Spudis, Volcanism on Mars, *Rev. Geophys.*, *19*, 13–41, 1981.

Greeley, R., and B. D. Schneid, Magma generation on Mars: Amounts, rates, and comparisons with Earth, Moon, and Venus, *Science*, *254*, 996–998, 1991.

Gregg, T. K. P., and J. H. Fink, Variations in lava flow width related to effusion rates through laboratory simulations, *Lunar Planet. Sci. Conf.*, *28*, 461–462, 1997.

Gregg, T. K. P., D. A. Crown, and R. Greeley, Geologic map of MTM quadrangle -20252, Tyrrhena Patera region of Mars, *U.S. Geol. Surv. Misc. Invest. Ser. Map, I-2556*, 1998.

Gudmundsson, A., Formation of collapse calderas, *Geology*, *16*, 808–810, 1988.

Gulick, V. C., and V. R. Baker, Origin and evolution of valleys on Martian volcanoes, *J. Geophys. Res.*, *95*, 14325–14344, 1990.

Harris, S. A., The aureole of Olympus Mons, *J. Geophys. Res.*, *82*, 3099–3107, 1977.

Harvey, R. P., and H. Y. McSween, The parent magma of the Nakhlite meteorites: Clues from melt inclusions, *Earth Planet. Sci. Lett.*, *82*, 3099–3107, 1977.

Head, J. W., and L. Wilson, Basaltic pyroclastic eruptions: Influence of gas-release patterns and volume fluxes on fountain structure, and the formation of cinder cones, spatter cones, rootless flows, lava ponds and lava flows, *J. Volcanol. Geotherm. Res.*, *37*, 261–271, 1989.

Head, J. W., M. Settle, and C. A. Wood, Origin of the Olympus Mons escarpment by erosion of pre-volcano substrate, *Nature*, *263*, 667–668, 1976.

Hodges, C. A., and H. J. Moore, The subglacial birth of Olympus Mons and its aureoles, *J. Geophys. Res.*, *84*, 8061–8074, 1979.

Hodges, C. A., and H. J. Moore, Atlas of volcanic landforms on Mars, *U.S. Geol. Surv. Prof. Pap.*, *1534*, 61–70, 1994.

Hulme, G., The dependence of the rheological properties and effusion rate of an Olympus Mons lava, *Icarus*, *27*, 207–213, 1976.

Hviid, S. F., M. B. Madsen, H. P. Gunnlaugsson, W., Goetz, J. M. Knudsen, R. B. Hargraves, P. Smith, D. Britt, A. R. Dinesen, C. T. Mogensen, M. Olsen, C. T. Pederson, and L. Vistisen, Magnetic properties experiments on the Mars Pathfinder lander: Preliminary results, *Science*, *278*, 1768–1770, 1997.

Jagoutz, E., H. Palme, H. Baddenhausen, K. Blum, M. Cendales, G. Dreibus, B. Spettel, V. Lorenz, and H. Wanke, The abundance of major, minor, and trace elements in the Earth's mantle as derived from primitive ultramafic nodules, *Proc. Lunar Planet. Sci.*, *10*, 2031–2050, 1979.

Johnson, M. C., M. J. Rutherford, and P. C. Hess, Chassigny petrogenesis: Melt compositions, intensive parameters, and water contents of Martian (?) magmas, *Geochem. Cosmochim. Acta*, *55*, 349–366, 1991.

Johnson, M. C., A. T. Anderson, Jr., and M. J. Rutherford, Pre-eruptive volatile contents of magmas, in *Volatiles in Magmas, Reviews in Mineralogy*, edited by M. R. Carroll and J. R. Holloway, Mineralogical Society of America, Washington, *30*, 281–330, 1994.

Kieffer, H. H., T. Z. Martin, A. R. Peterfreund, B. M. Jakosky, E. D. Miner, and F. D. Palluconi, Thermal and albedo mapping of Mars during the Viking primary mission, *J. Geophys. Res.*, *82*, 4249–4291, 1977.

King, E. A., Geologic map of the Mare Tyrrhenum quadrangle of Mars, *U.S. Geol. Surv. Misc. Invest. Ser. Map, I-1073*, 1978.

King, J. S., and J. R. Riehle, A proposed origin for the Olympus Mons escarpment, *Icarus*, *23*, 300–317, 1974.

Longhi, J., and V. Pan, The parent magmas of the SNC meteorites, *Proc. Lunar Planet. Sci.*, *19*, 451–464, 1989.

Longhi, J., E. Knittle, J. R. Holloway, and H. Wanke, The bulk composition, mineralogy and internal structure of Mars, in *Mars*, edited by H. H. Kieffer, B. M. Jakosky, C. W. Snyder, and M. S. Matthews, pp. 184–208, University of Arizona Press, Tucson, 1992.

Lopes, R. M. C., and C. R. J. Kilburn, Emplacement of lava flow fields:Application of terrestrial studies to Alba Patera, Mars, *J. Geophys. Res.*, *95*, 14383–14397, 1990.

Lopes, R. M. C., J. E. Guest, K. H. Hiller, and G. P. O. Neukum, Further evidence for mass movement origin of the Olympus Mons aureole, *J. Geophys. Res.*, *87*, 9917–9928, 1982.

Malin, M. C., Comparison of volcanic features of Elysium (Mars) and Tibesti (Earth), *Geol. Soc. Am. Bull.*, *88*, 909–919, 1977.

Malin, M. C., Lengths of Hawaiian lava flows, *Geology*, *8*, 306–308, 1980.

Masursky, H., R. M. Batson, J. F. McCauley, L. A. Soderblom, R. L. Wildey, M. H. Carr, D. J. Milton, D. E. Wilhelms, B. A. Smith, T. B. Kirby, J. C. Robinson, C. B. Levoy, G. A. Briggs, T. C. Duxbury, C. H. Acton, B. C. Murray, J. A. Cutts, R. P. Sharp, S. Smith, R. B. Leighton, C. Sagan, J. Veverka, M. Noland, G. DeVaucoulerus, M. Davies, and A. T. Young, Mariner 9 television reconnaissance of Mars and its satellites: Preliminary results, *Science*, *175*, 294–304, 1972.

McCauley, J. F., M. H. Carr, J. A. Cutts, W. K. Hartmann, H. Masursky, D. J. Milton, R. P. Sharp, and D. E. Wilhelms, Preliminary Mariner 9 report on the geology of Mars, *Icarus*, *17*, 289–327, 1972.

McCoy, T. J., G. J. Taylor, and K. Keil, Zagami: Product of a two-stage magmatic history, *Geochim. Cosmochim. Acta*, *56*, 3571–3582, 1992.

McGetchin, T. R., and J. R. Smyth, The mantle of Mars: Some possible geological implications of its high density, *Icarus*, *34*, 512–536, 1978.

McGuire, W. J., Volcano instability: A review of contemporary themes, in *Volcano Instability on Earth and Other Planets*, pp. 1–23, Geol. Soc. London Spec. Publ., 1996.

McSween, H. Y., What we have learned about Mars from SNC meteorites, *Meteoritics*, *29*, 757–779, 1994.

McSween, H. Y., and R. P. Harvey, Outgassed water on Mars: Constraints from melt inclusions in SNC meteorites, *Science*, *259*, 1890–1892, 1993.

McSween, H. Y., Jr., S. L. Murchie, J. A. Crisp, N. T. Bridges, R. C. Anderson, J. F. Bell III, D. T. Britt, J. Bruckner, G. Dreibus, T. Economou, A. Ghosh, M. P. Golombek, J. P. Greenwood, J. R. Johnson, H. J. Moore, R. V. Morris, T. J. Parker, R. Rieder, R. Singer, and H. Wanke, Chemical, multispectral, and textural constraints on the composition and origin of rocks at the Mars Pathfinder landing site, *J. Geophys. Res.*, *104*, 8679–8715, 1999.

Moore, H. J., D. W. G. Arthur, and G. G. Schaber, Yield strengths of flows on the Earth, Mars, and Moon, *Proc. Lunar Planet. Sci.*, *9*, 3351–3378, 1978.

Moore, J. G., D. A. Clauge, R. T. Holcomb, P. W. Lipman, W. R. Normark, and M. E. Torresan, Prodigious submarine landslides on the Hawaiian ridge, *J. Geophys. Res.*, *94*, 17465–17484, 1989.

Morgan, J. W., and E. Anders, Chemical composition of Mars, *Geochim. Cosmochim. Acta*, *43*, 1601–1610, 1979.

Morris, E. C., Aureole deposits of the Martian volcano Olympus Mons, *J. Geophys. Res.*, *87*, 1164–1178, 1982.

Mouginis-Mark, P. J., Volcano/ground ice interactions in Elysium Planitia, Mars, *Icarus*, *64*, 265–284, 1985.

Mouginis-Mark, P. J., The influence of oceans on Martian volcanism, *Lunar Planet. Sci.*, *24*, 1021–1022, 1993.

Mouginis-Mark, P. J., and M. S. Robinson, Evolution of the Olympus Mons caldera, Mars, *Bull. Volcanol.*, *54*, 347–360, 1992.

Mouginis-Mark, P. J., and M. Tatsumura-Yoshioka, The long lava flows of Elysium Planitia, Mars, *J. Geophys. Res.*, *103*, 19389–19400, 1998.

Mouginis-Mark, P. J., L. Wilson, and J. W. Head, Explosive volcanism on Hecates Tholus, Mars; Investigation of eruption conditions, *J. Geophys. Res.*, *87*, 9890–9904, 1982.

Mouginis-Mark, P. J., L. Wilson, J. W. Head, H. Brown-Steven, J. L. Hall, and K. D. Sullivan, Elysium Planitia, Mars: Regional geology, volcanology, and evidence for volcano–ground ice interactions, *Earth Moon Planets*, *30*, 149–173, 1984.

Mouginis-Mark, P. J., L. Wilson, and J. R. Zimbelman, Polygenic eruptions on Alba Patera, Mars, *Bull. Volcanol.*, *50*, 361–379, 1988.

Muhleman, D. O., A. W. Grossman, B. J. Butler, and M. A. Slade, Radar images of Mars, *Science*, *253*, 1508–1513, 1991.

Neukum, G., and K. Hiller, Martian ages, *J. Geophys. Res.*, *86*, 3097–3121, 1981.

Owen, T., The composition and early history of the atmosphere of Mars, in *Mars*, edited by H. H. Kieffer, B. M. Jakosky, C. W. Snyder, and M. S. Matthews, pp. 818–834, University of Arizona Press, Tucson, 1992.

Parker, T. J., D. S. Gorsline, R. S. Saunders, D. C. Pieri, and D. M. Schneeberger, Coastal geomorphology of the Martian northern plains, *J. Geophys. Res.*, *98*, 11061–11078, 1993.

Peterson, J. E., Geologic map of the Noachis quadrangle of Mars, *U.S. Geol. Surv. Misc. Invest. Ser. Map*, *I-910*, 1977.

Peterson, J. E., Volcanism in the Noachis–Hellas region of Mars, 2, *Proc. Lunar Planet. Sci.*, *9*, 3411–3432, 1978.

Plescia, J. B., The Tempe volcanic province of Mars and comparisons with the Snake River Plains of Idaho, *Icarus*, *45*, 586–601, 1981.

Plescia, J. B., An assessment of volatile release from recent volcanism in Elysium, Mars, *Icarus*, *104*, 20–32, 1993.

Plescia, J. B., and R. S. Saunders, The chronology of the Martian volcanoes, *Proc. Lunar Planet. Sci.*, *10*, 2841–2859, 1979.

Pollack, J. B., T. Roush, F. Witteborn, J. Bregman, D. Wooden, C. Stoker, O. B. Toon, D. Rank, B. Dalton, and R. Freedman, Thermal emission spectra of Mars (5.4–10.5 μm): Evidence for sulfates, carbonates, and hydrates, *J. Geophys. Res.*, *95*, 14595–14628, 1990.

Popp, R. K., D. Virgo, and W. Phillips-Michael, H deficiency in kaersutitic amphiboles: Experimental verification, *Am. Mineral.*, *80*,. 1347–1350, 1995.

Potter, D. B., Geologic map of the Hellas quadrangle of Mars, *U.S. Geol. Surv. Misc. Invest. Ser. Map*, *I-941*, 1976.

Reimers, P. E., and P. D. Komar, Evidence for explosive volcanic density currents on certain Martian volcanoes, *Icarus*, *39*, 88–110, 1979.

Rieder, R., T. Economou, H. Wänke, A. Turkevich, J. Crisp, J. Brückner, G. Dreibus, and H. Y. McSween, Jr., The chemical composition of Martian soil and rocks returned by the mobile alpha proton X-ray spectrometer: Preliminary results from the X-ray mode, *Science*, *278*, 1771–1774, 1997.

Robinson, M. S., and S. K. Rowland, Evidence for large scale sector collapse at Tharsis Tholus, in *Conf. Volcano Instability Earth and Other Planets*, p. 44, Geological Society of London, 1994.

Robinson, M. S., P. J. Mouginis-Mark, J. R. Zimbelman, S. S. C. Wu, K. K. Ablin, and A. E. Howtington-Kraus, Chronology, eruption duration, and atmospheric contribution of the Martian volcano Apollinaris Patera, *Icarus*, *104*, 301–323, 1993.

Rubin, A. M., and D. D. Pollard, Origins of blade-like dikes in volcanic rift zones, in *Volcanism in Hawaii*, edited by R. W. Decker, T. L. Wright, and P. H. Stauffer, pp. 1449–1470, *U.S. Geol. Surv. Prof. Pap.*, *1350*, 1987.

Schneeberger, D. M., and D. C. Pieri, Geomorphology and stratigraphy of Alba Patera, Mars, *J. Geophys. Res.*, *96*, 1907–1930, 1991.

Schubert, G., S. C. Solomon, D. L. Turcotte, M. J. Drake, and N. H. Sleep, Origin and thermal evolution of Mars, in *Mars*, edited by H. H. Kieffer, B. M. Jakosky, C. W. Snyder, and M. S. Matthews, pp. 147–183, University of Arizona Press, Tucson, 1992.

Scott, D. H., Volcanoes and volcanic provinces: Martian western hemisphere, *J. Geophys. Res.*, *87*, 9839–9851, 1982.

Scott, D. H., and K. L. Tanaka, Mars: A large highland volcanic province revealed by Viking images, *Proc. Lunar Planet. Sci.*, *12*, 1449–1458, 1981.

Scott, D. H., and K. L. Tanaka, Geologic map of the western equatorial region of Mars, *U.S. Geol. Surv. Misc. Invest. Map*, *I-1802-A*, 1986.

Smith, D. E., M. T. Zuber, H. V. Frey, J. B. Garvin, J. W. Head, D. O. Muhleman, H. J. Zwally, W. B. Banerdt, T. C. Duxbury, G. H. Pettengill, R. O. Phillips, and S. C. Solomon, Topography of the northern hemisphere of Mars from the Mars Orbiter Laser Altimeter, *Science*, *279*, 1686–1692, 1998.

Smith, P. H., J. F. Bell III, N. T. Bridges, D. T. Britt, L. Gaddis, R. Greeley, H. Kueller, K. E. Herkenhoff, R. Jaumann, J. R. Johnson, R. L. Kirk, M. Lemmon, J. N. Maki, M. C. Malin, S. L. Murchie, J. Oberst, T. J. Parker, R. J. Reid, R. Sablotny, L. A. Soderblom, C. Stoker, R. Sullivan, N. Thomas, M. G. Tomasko, W. Ward, and E. Wegryn, Results from the Mars Pathfinder camera, *Science*, *278*, 1758–1765, 1997.

Soderblom, L. A., Historical variations in the density and distribution of impacting debris in the inner solar system: Evidence from planetary imaging, in *Impact and Explosion Cratering*, edited by D. J. Roddy, R. O. Pepin, and R. B. Merrill, pp. 629–633, Pergamon Press, New York, 1977.

Soderblom, L. A., The composition and mineralogy of the Martian surface from spectroscopic observations: 0.3 mm to 50 mm, in *Mars*, edited by H. H. Kieffer, B. J. Jakosky, C. W. Snyder, and M. S. Matthews, pp. 557–593, University of Arizona Press, Tucson, 1992.

Sparks, R. S. J., The dynamics of bubble generation and growth in magmas: A review and analysis, *J. Volcanol. Geotherm. Res.*, *3*, 1–37, 1978.

Squyres, S. W., D. E. Wilhelms, and A. C. Moosman, Large-scale volcano–ground ice interactions on Mars, *Icarus*, *70*, 385–408, 1987.

Tanaka, K. L., Ice-lubricated gravity spreading of the Olympus Mons aureole deposit, *Icarus*, *62*, 191–206, 1985.

Tanaka, K. L., and D. H. Scott, Geologic map of the polar regions of Mars, *U.S. Geol. Surv. Misc. Invest. Ser. Map*, *I-1802-C*, 1987.

Tanaka, K. L., N. K. Isbell, D. H. Scott, R. Greeley, and J. E. Guest, The resurfacing history of Mars: A synthesis of digitized, Viking-based geology, *Proc. Lunar Planet. Sci.*, *18*, 665–678, 1988.

Treiman, A. H., The parent magma of the Nakhla (SNC) meteorite, inferred from magmatic inclusions, *Geochim. Cosmochim. Acta*, *57*, 4753–4767, 1993.

Walker, G. P. L., Lengths of lava flows, *Philos. Trans. R. Soc. London Ser. A*, *274*, 107–118, 1973.

Weidenschilling, S. J., Accretion of the terrestrial planets. II, *Icarus*, *27*, 161–170, 1976.

Whitford-Stark, J. L., Factors influencing the morphology of volcanic landforms: An Earth–Moon comparison, *Earth Sci. Rev.*, *18*, 109–168, 1982.

Wilson, L., and J. W. Head, A comparison of volcanic eruption processes on Earth, Moon, Mars, Io, and Venus, *Nature*, *302*, 663–669, 1983.

Wilson, L., and J. W. Head, Factors controlling the structures of magma chambers in basaltic volcanoes, *Lunar Planet. Sci.*, *21*, 1343–1344, 1990.

Wilson, L., and J. W. Head, Mars: Review and analysis of volcanic eruption theory and relationships to observed landforms, *Rev. Geophys.*, *32*, 221–263, 1994.

Wilson, L., S. J. Sparks, T. C. Huang, and N. D. Watkins, The control of volcanic column heights by eruption energetics and dynamics, *J. Geophys. Res.*, *83*, 1829–1836, 1978.

Wilson, L., J. W. Head, and P. J. Mouginis-Mark, Theoretical analysis of Martian volcanic eruption mechanisms, in *The Planet Mars*, *ESA SP-185*, pp. 107–113, Leeds, UK, 1982.

Wise, D. U., Geologic map of the Arcadia quadrangle of Mars, *U.S. Geol. Surv. Misc. Invest. Ser. Map*, *I-1154*, 1979.

Wood, B. J., A. Pawley, and D. R. Frost, Water and carbon in the Earth's mantle, *Philos. Trans. R. Soc. London Ser. A*, *354*, 1495–1511, 1996.

Wood, C. A., Monogenetic volcanoes of the terrestrial planets, *Proc. Lunar Planet. Sci. Conf.*, *10*, 2815–2840, 1979.

Wood, C. A., Calderas: A planetary perspective, *J. Geophys. Res.*, *89*, 8391–8406, 1984.

Zimbelman, J. R., Estimates of rheologic properties for flows on the Martian volcano Ascraeus Mons, Proc. Lunar Planet. Sci. Conf. 16, in *J. Geophys. Res.*, *90 (suppl.)*, D157–D162, 1985.

Zuber, M. T., and P. J. Mouginis-Mark, Caldera subsidence and magma chamber depth of the Olympus Mons volcano, Mars, *J. Geophys. Res.*, *97*, 18295–18307, 1992.